

**Assessment of the hydro-geo-chemistry
of a polluted coastal aquifer in Scotland**

Angela Duerden

This thesis is submitted in part fulfillment of the requirements for the BSC. Degree in
Environmental Science at the University of Lancaster, December 2002

Acknowledgments

I would firstly like to acknowledge and thank my parents for their ongoing support and for enabling me to go to University. My sincere thanks go to my supervisor, Dr. Andrew Binley, for his support and advice in the field and during the writing up of this study. I would also like to thank Peter Winship for his help in the field and with the downloaded data and for getting me to Scotland in the first place!

I would like to thank Ann Wilkinson for organizing and helping me to prepare the sampling equipment and for the use of the laboratory.

I would also like to thank Patricia Enot, Edinburgh University, for her guidance and knowledge of the field site and the passing on of her skills with respect to sampling methods.

Abstract

The hydrogeochemical processes that occur in coastal aquifers are affected by the influx and discharge of saline water into or out of the groundwater system at periodic times during tidal cycles. When a landfill is located over a coastal estuary leachate that is produced may enter the sea through submarine groundwater connections in the aquifer. The geochemical interactions that occur in this leachate are affected by prevailing conditions of pH, the geology of the aquifer and interactions between seawater and freshwater.

The periodic cycling of seawater in a coastal aquifer can cause the movement of a pollutant plume towards an estuary during low tides but this movement should be countered when there is an influx of fresh seawater at high tides. At the Ardeer ICI landfill site in Scotland, the hydraulic setting of the landfill is near to the estuary of the River Garnock, which causes groundwater to discharge towards the estuary at low tide. However, the Scottish coastline is less than a kilometer west of the site and this may have the effect that water will flow towards the estuary even at high tide. This will influence the movement of a leachate plume, which will eventually reach the estuary and cause a pollution incident. The direction of groundwater flow during neap tides is not affected by high and low tides but it needs to be determined that there is a directional change when a spring tide occurs.

The layering of the aquifer shows that the hydraulic conductivity of the gravel layer found at 6 to 8m may be higher than that of the sands found above and below this layer. Other research on coastal aquifers has shown that submarine groundwater discharge into the sea can account for as much as 40% of the total river input to the sea (Li and Barry, 1999), and so the concentration of the leachate, identified by sampling for zinc, in the upper metres of the landfill may be diluted by freshwater flowing through the gravel layer. The spring and neap tidal cycling affected the groundwater temperatures of the aquifer but there did not appear to be any effects on the geochemistry of zinc in the upper metres of the aquifer.

Contents

<u>ABSTRACT</u>	3
<u>1. INTRODUCTION</u>	6
<u>1.1. THE TIDES AND THEIR HYDROLOGICAL EFFECTS</u>	6
<u>1.2. TIDAL PUMPING EFFECTS ON GROUNDWATER CHEMISTRY</u>	8
<u>2. PROBLEM DESCRIPTION AND PROJECT AIMS</u>	8
<u>2.1. GEOLOGY</u>	10
<u>2.2. COMPLETION DETAILS OF THE BOREHOLES</u>	13
<u>2.3. PREVIOUS RESEARCH AT THE SITE</u>	13
<u>2.4. AIMS</u>	15
<u>3. METHOD</u>	16
<u>3.1. IN-SITU MONITORING</u>	16
<u>3.1.1. Head Measurements</u>	16
<u>3.1.2. Slug-testing in ALO3</u>	16
<u>3.1.3. Vertical Chemical Profiles in ALO3</u>	17
<u>3.1.4. Continuous data logging of Temperature, pH and Electrical Conductivity in ALO3</u>	17
<u>3.2. GROUNDWATER AND SURFACE WATER SAMPLING</u>	17
<u>3.2.1. Multilevel sampling boreholes (MLS)</u>	17
<u>3.2.2. Estuarine Sampling</u>	17
<u>3.2.3. Filtration of groundwater samples</u>	18
<u>3.4. ATOMIC ABSORPTION SPECTROSCOPY</u>	19
<u>3.4.1. Advantages</u>	19
<u>3.4.2. Disadvantages</u>	19
<u>3.4.3. Analytical Technique</u>	20
<u>3.5. FLAME EMISSION SPECTROSCOPY</u>	20
<u>3.5.1. Advantages</u>	20
<u>3.5.2. Disadvantages</u>	21
<u>3.5.3. Analytical Technique</u>	21
<u>4. RESULTS</u>	21
<u>4.1.1 FLUCTUATIONS IN THE WATER TABLE</u>	21
<u>4.1.2 HYDRAULIC CONDUCTIVITY OF THE AQUIFER</u>	23
<u>4.2 GEOCHEMICAL VARIATIONS IN THE AQUIFER</u>	25
<u>4.2.1 ALO3 Borehole</u>	25
<u>4.2.1.1 Vertical Chemical Profile</u>	25
<u>4.2.1.2 Monitoring of electrical conductivity, temperature and pH</u>	26
<u>4.2.3 MLS Boreholes</u>	29
<u>4.2.3.1 Daily spatial variations</u>	29
<u>4.2.3.2 Temporal variations</u>	33
<u>5. DISCUSSION</u>	37

<u>5.1 HYDRAULIC CHARACTERISTICS OF THE SANDSTONE AQUIFER</u>	37
<u>5.2 GEOCHEMICAL INTERACTIONS</u>	38
<u>6. CONCLUSION</u>	40
<u>7. ERRORS AND IMPROVEMENTS</u>	41
<u>8. REFERENCES</u>	42
<u>APPENDICES</u>	43
<u>APPENDIX 1 – THE COMPLETION OF THE MLS BOREHOLES</u>	43
<u>APPENDIX 2 – THE COMPLETION OF THE AL BOREHOLES</u>	43
<u>APPENDIX 3 – PREVIOUS DATA FROM THE SITE</u>	45
<u>Head Monitoring</u>	45
<u>Temperature monitoring</u>	45
<u>Electrical conductivity monitoring</u>	46
<u>APPENDIX 4 – SAMPLING AND FILTRATION METHODS</u>	46
<u>APPENDIX 5 – ANALYTICAL METHODS USED FOR AAS AND EMS</u>	49
<u>APPENDIX 6 – CORRECTION DETAILS</u>	50

1. Introduction

As the population and their overall contribution to the amount of waste material that is generated increases, the processing and disposal methods of waste are becoming increasingly important. The need to ensure that there are adequate measures in place to minimize the mobility of leachate created in these landfills is now being realized in an effort to prevent groundwater pollution.

Many municipal landfill sites are found in coastal areas where large towns and cities are found, e.g. Morecambe and Lancaster. Certain older industrial complexes may have dumped their industrial waste in company-owned landfills, such as the ICI site at Ardeer in Scotland. These landfills all store waste material that can be biologically or chemically broken down. The by-products and end products of these reactions can be more harmful than the initial contaminant. The breakdown processes can produce a leachate solution that can combine with precipitation on the site and a toxic solution will migrate to the bottom of the landfill. In landfills that are lined, this leachate is essentially trapped and prevented from migrating into the groundwater. However, some older landfill sites are not sufficiently lined, if at all, and the leachate becomes a pollutant plume that migrates through the groundwater. It can be difficult to monitor the movement of these plumes because the leachate consists of many different compounds, including products of chemical reactions that have already occurred within the landfill, that all react differently in the water column. Heavier hydrocarbons, for example, sink through the saturated zone and gather where an impermeable layer prevents further downward movement.

Many of these landfills are situated on coastal aquifers that are intensively used for drinking water supplies. It has been noted that there are fluctuations in the groundwater levels due to the tidal cycling near the coast, with a higher water table at high tide than the water level of the same point at low tide. There are also geochemical effects that occur when saline water and freshwater meet (refer to Appelo, 1994). Appelo discovered that when freshwater flows into a saline aquifer there are interactions between calcium, magnesium, sodium and the aquifer material. There are initial increases in sodium in solution while calcium and magnesium concentrations decrease. It has also been found by Li et al. (1999) that there are significant cycling effects of coastal waters within and between freshwater aquifers and the oceans. This may have significant effects on the amount of pollution that enters saline environments.

1.1. The tides and their hydrological effects

The Moon and the Sun affect the movement of water on the surface of the planet i.e. in the oceans. The effect of the rotation of the Earth, as it moves along its orbit around the sun, causes shallower water at the poles and deeper water at the equator. The Moon has a gravitational effect on the water in the oceans as well.

The Earth-Moon effect on the water in the oceans is the greater of the two interactions because the distance between them is smaller than between the Earth and the Sun. The Moon revolves around the Earth once every 28 days and causes the water in the oceans to rise when directly over-head. This leads to a decrease in the height of water at the

opposite side of the planet. These pulls on the height of the water occur every 12 hours and 25 minutes and this creates a wave that generates a tide called the M2 tide. This effect can be magnified by resonance of the wave by land barriers, which occurs in the North Atlantic Ocean. Another wave then travels around the North Atlantic Basin and when it interacts with the coastal shelf off the European continent it causes an increase in seawater height and the water velocity increases. This causes the tides that then ebb away as the wave moves through the Basin. The tides are high when the Moon is directly overhead (refer to Tett, n.d.).

The Earth-Sun effect occurs every 12 hours but has a smaller net effect than that of the Earth-Moon interaction. The S2 tide is created as a result of this interaction and also resonates around the North Sea Basin.

When the two tides are in phase, their effects combine and give a higher high water mark than the average height. This is called a Spring tide. The two tides can also be out of phase and because the water is moving in two separate directions there is a much lower tide generated, this is called the Neap tide. The two cycles can be seen in Figure 1.

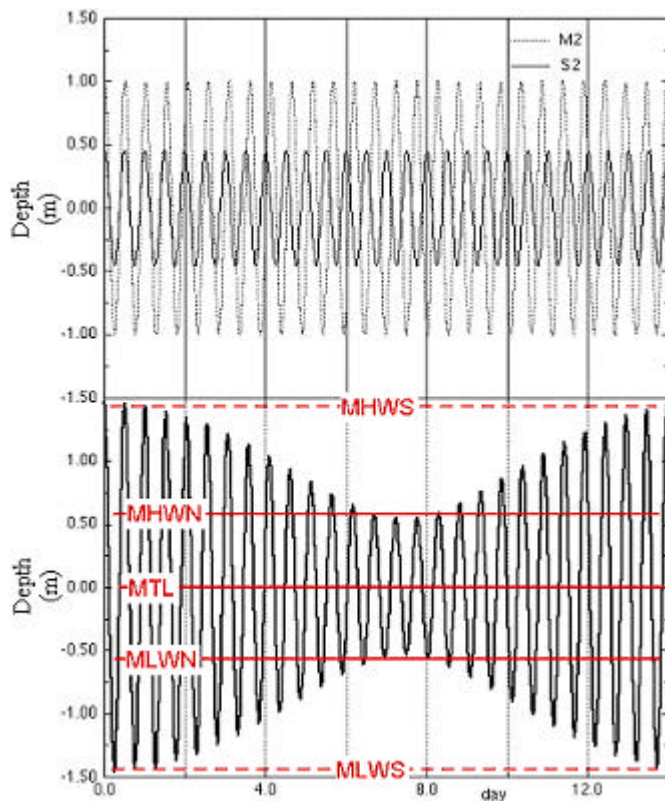


Figure 1: Neap and spring tidal heights. MTL is the Mean Tide Level, MHWS is the Mean High Water Spring tide, MLWS is the Mean Low Water Spring tide, MHWN is the Mean High Water Neap tide and MLWN is the Mean Low Water Neap tide (taken from Tett, n.d).

It can be seen in Figure 1 that the combined height of the two waves, M2 and S2, is greatest when they are acting at the same time. The Spring tides have lower low water marks and higher high water marks.

The tides cause cycling of groundwater through the aquifer and there will be variations in the height of the water table as this occurs. This could change the groundwater velocity because there will be changes in the hydraulic gradients near the estuary.

1.2. Tidal pumping effects on groundwater chemistry

Recent research has been carried out that has linked the processes that occur in coastal aquifers to those that occur in terrestrial estuaries. The coastal aquifer has been termed a subterranean estuary (Appelo, 1994; Moore, 1999) because the interactions between saline water and freshwater that occur at high water tides are similar to the processes between various ions and sediment in terrestrial estuaries.

Appelo (1994) has shown that there are adsorption/desorption reactions involved when seawater is flushed out of the pores by the influx of fresh water, for example when the tides are ebbing. There are higher concentrations of sodium (Na^{2+}), magnesium (Mg^{2+}) and potassium (K^+) in seawater than in fresh water and when an influx of freshwater occurs these excess cations are lost from the surface of aquifer particles in an order of their relative affinity for adsorption onto the particles.

The pH of groundwater has been linked to the concentrations of many heavy metals, such as zinc (Zn), manganese (Mn), chromium (Cr) and aluminium (Al) etc. Johnson et al. (2000) have shown that the oxidation of sulphide minerals in the Nickel Rim tailings impoundment has produced water of very low pH. It has been shown that the lower the pH of the groundwater then the more desorption of metals that occurs off the sediment, with greater concentrations of dissolved metals in the groundwater (refer to Gee et al., 2001; Jurjovec et al., 2002; Johnson et al., 2000).

It is considered that the majority of freshwater that is discharged into the oceans consists of groundwater that flows through the coastal aquifer and then subsequent seepage into the sea (Li et al., 1999). This can determine the rate of transport of chemicals to the oceans that may detrimentally affect the marine environment.

2. Problem description and project aims

An aquifer on the western coast of Scotland was chosen as a good site to investigate the processes that occur in polluted aquifer areas when they are in close proximity to estuaries. The site is located on a landfill at the ICI Ardeer Explosives site near Stevenston (refer to Figure 2).

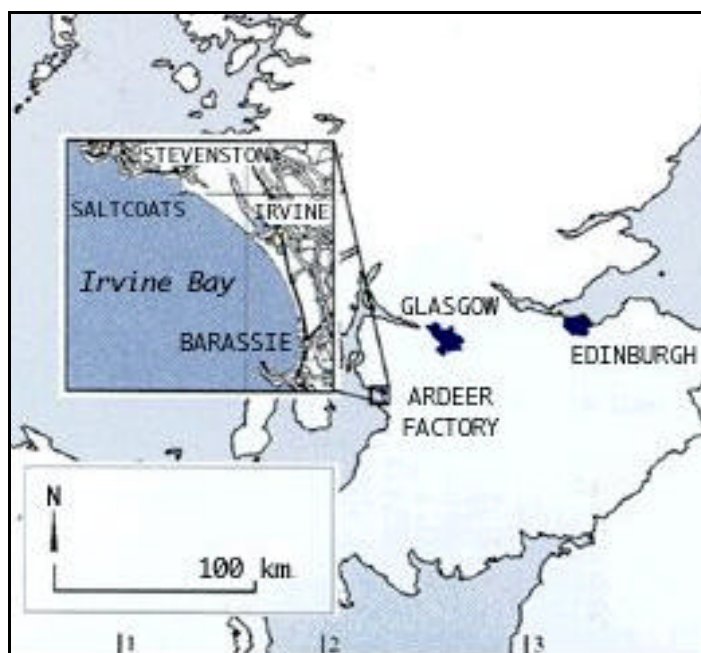


Figure 2: A map of Scotland showing the location of the ICI Ardeer site near Stevenston (refer to Dolan, n.d.)

The site at Ardeer opened in January, 1873, with the initial production of dynamite for industrial purposes and since then has branched into the production of nitroglycerine, nitrocellulose, leather cloth, lacquers, safety fuses, black powder, detonators, Cellofas (a cellulose derivative) and silicones (refer to Clements, n.d.). There is an active research department onsite that is constantly forming new products for sale internationally.

The site developed its own landfills to dispose of industrial waste. These landfills were sited in the sand dunes near the estuary, where the River Garnock enters the sea. These sand dunes had previously been stabilized in the early stages of development of the site using ashes and planting hardy grass that would colonise the dunes.

The landfill is close to the estuary and is affected by the tidal effect on the movement of water through the underlying aquifer. The landfill is very shallow (approximately 6m), and with evidence that shows that the water table height varies from 2.9-3.3m, then leachate from the area can drain into the estuary.

The leachate consists of a range of dissolved metals such as zinc, manganese, magnesium, nickel, copper, chromium and aluminium. The previous chemical analyses show that aluminium, iron, zinc and calcium are the major elements that are found at very high levels in the top few metres of the landfill. The direction of the movement of the leachate from the landfill, through the underlying rock, will be affected by the groundwater flow direction and the underlying geology. It has been seen that there has not been any effect of the landfill on the quality of water in the estuary so there may be hydraulic processes that affect the distance that the plume travels.

2.1. Geology

The landfill area contains nine boreholes. These are shown in Figure 3.

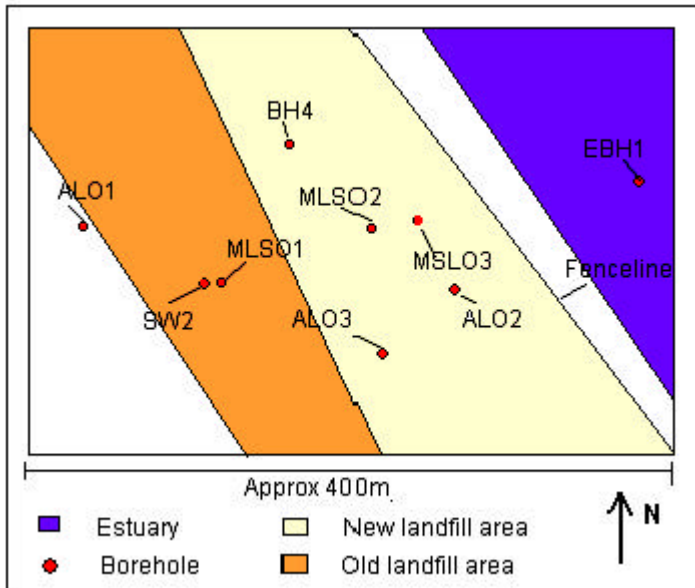


Figure 3: Site plan showing the location of the boreholes and the landfill areas

Geological profiles of the boreholes were plotted during the drilling process and were used to determine the geology of the landfill site. These are illustrated below in Figure 4 and 5. It must be noted that there is disturbance of the geological sequence during drilling and the depths can only be approximations.

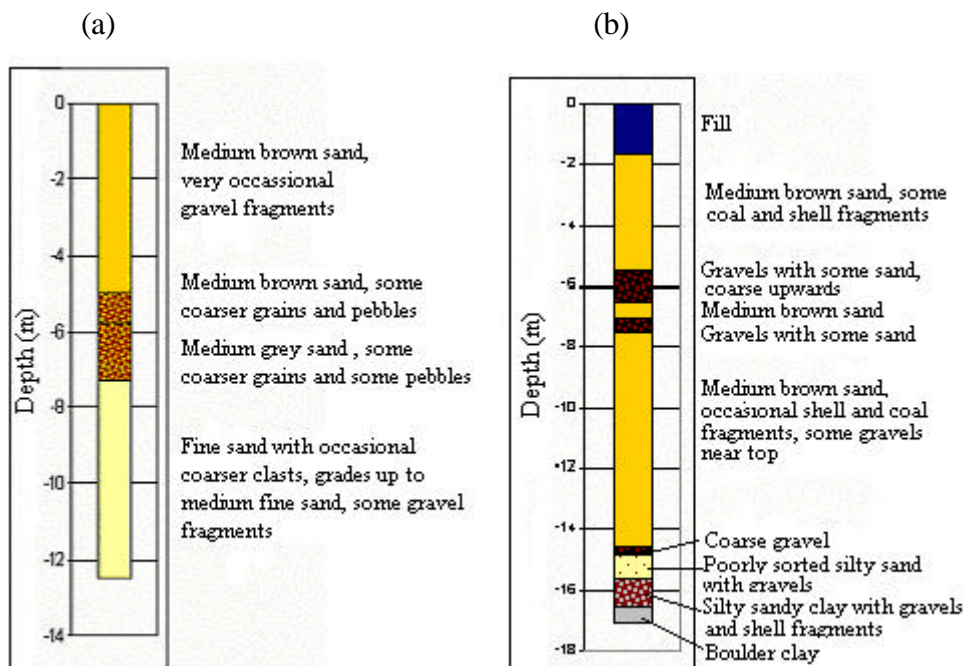


Figure 4: Geological profiles of the (a) ALO1 and (b) MLSO1 boreholes (after Winship, pers. comm., n.d.).

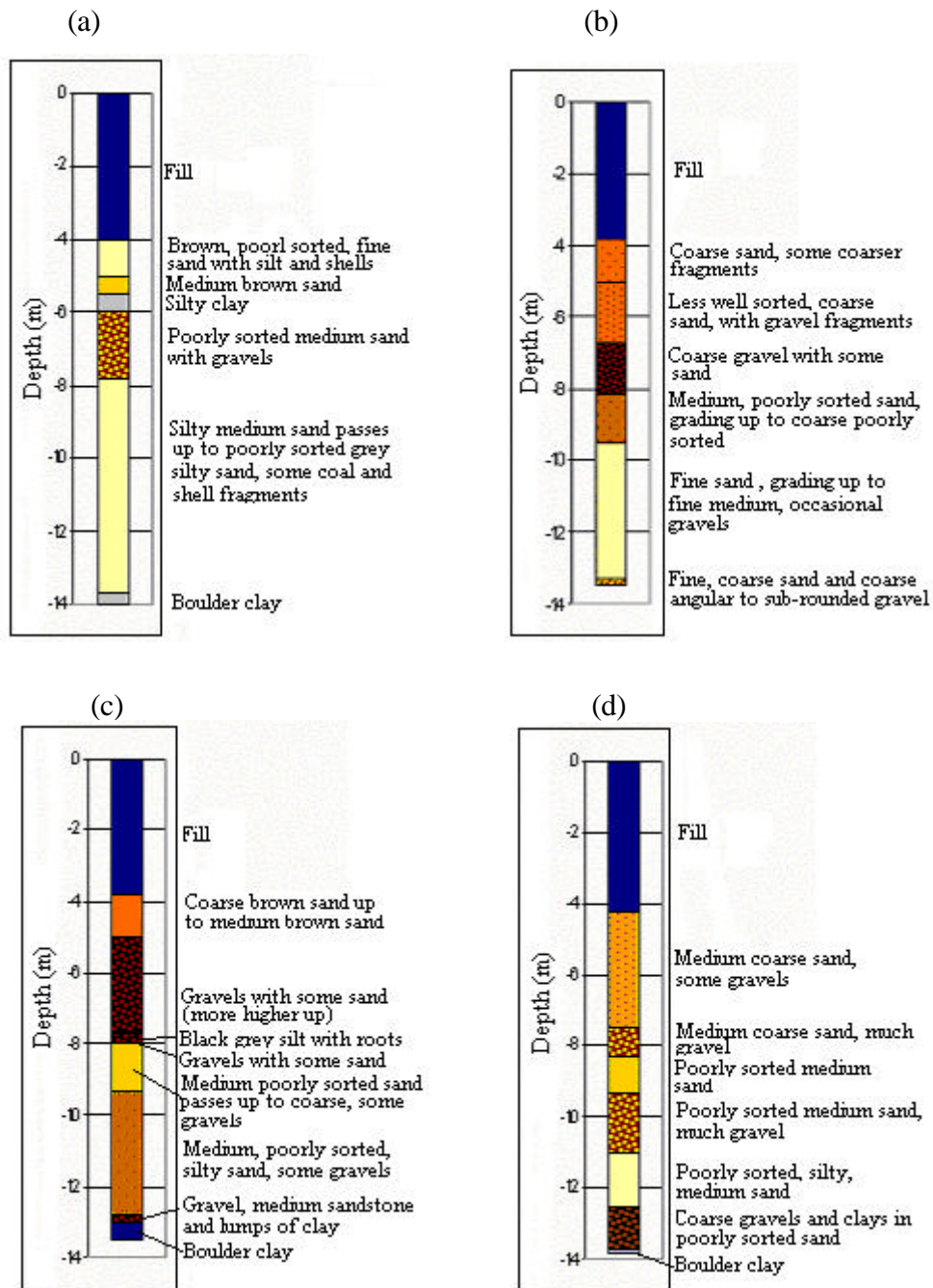


Figure 5: Geological profiles of the MLS and AL boreholes on the landfill (after Winship, pers. comm., n.d.). The boreholes are labelled as follows (a) MLSO2, (b) ALO3, (c) MLSO£, (d) ALO2.

The underlying geology consists of sandstones that are interspersed with layers of gravels. A description of each of the boreholes is given below (Winship, pers. comm. n.d.):-

- ALO1 is farthest away from the estuary, is drilled to a depth of 12.50m and has four main geological sequences. A layer of brown sand and pebbles (5-6m) underlies an

upper layer of brown sandstone (depth of 0-5m). The third layer consists of medium grey sand and pebbles (6-7.5m) and the final layer in the sequence contains fine sands, up to a coarse grain size, and some gravel (7.5-12.37m).

Old landfill

- MLSO1 has a maximum depth of 17.10m and is sampled to a depth of 16.4m (sample extraction from this last part is not possible with the equipment used). There is a sandstone layer that dominates the sequence, which is divided into three separate layers by two layers of gravel at depths of 5.5-6.5m and 7.0-7.5m. The final layers consist of clays and silt (15-17m).

New Landfill

- MLSO2 has a maximum depth of 14.0m and is sampled to a depth of 13.3m. The upper layer consists of brown sandstone with some shell fragments (4-5m) with a layer of medium brown sand underlying this (5.0-5.5m). There is a layer of silty clay at a depth of 5.5m, followed by a layer of sand and gravel (6-7.8m). A layer of silty medium sand (7.8-13.8m), consisting of more grey silty sand higher up the sequence, underlies this. The bottom layer of the drilled borehole is boulder clay.
- ALO3 is a similar distance from the estuary as MLSO2. The borehole has a maximum depth of 13.50m deep but the geological sequence in this borehole is different to MLSO2. There is more gravel than in the MLSO2 borehole and this will affect permeability and porosity. The initial layer consists of coarse sand (3.9-5.0m) which is followed by a layer of less sorted coarse sand and gravel (5-6.5m). A gravel layer with sand can be found at a depth of 6.5m and then sand layers are found again with gradually less gravel (8.0m-9.5m and 9.5m-13.0m).
- MLSO3 has a maximum depth of 13.50m and is sampled to a depth of 12.5m. The two sandstone layers of medium brown sand, that were seen in MLSO1, are present (3.8-5.0m and 8-9.3m), separated by gravels (5-7.5m) and a silty layer (7.5-8m), which appears to be a small local deposit. There is then a layer of medium silty sand and gravel (9.3-13.0m) and layers of gravel, mud and boulder clay underlie this.
- ALO2 is the borehole nearest to the estuary and has a maximum depth of 13.80m. The initial layer, 4.2-7.5m, consists of medium-coarse sand and some gravel and then the ratio of gravel to sand increases (7.5-8.2m). A layer of sand is found at 8.2m and then the amount of gravel increases again at 9.2-11m. A layer of silty sand (11-12.5m) overlies a layer of coarse gravels and clays (12.5-13.8m).

The vertical cross-section of the area from the ALO1 borehole to the estuary can be drawn up using the geological profiles from above. This is shown in Figure 6. The aquifer is unconfined and consists of two gravel sequences from the land surface that are split by a layer of clay with a lower electrical conductivity. The base of the aquifer is bounded by a clay layer, which can be assumed to act as an impermeable layer.

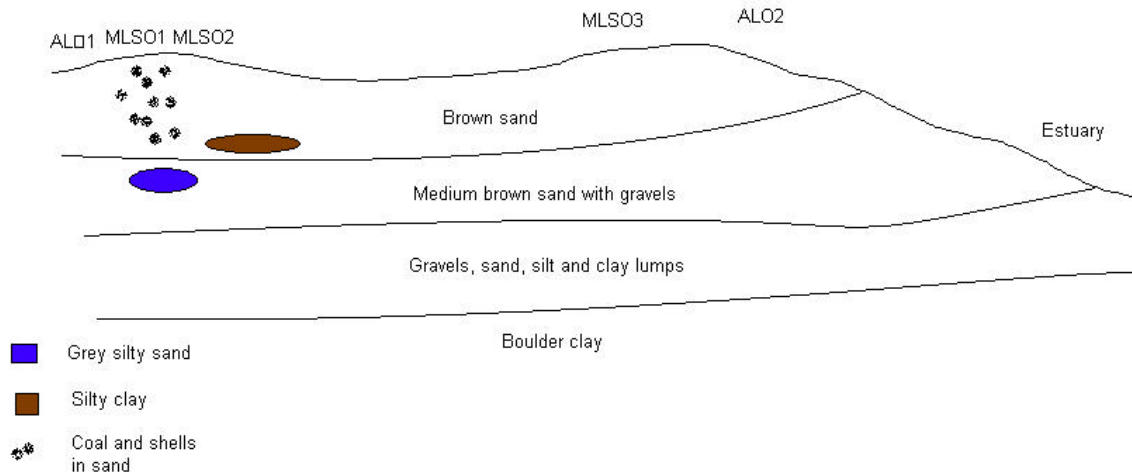


Figure 6: The horizontal cross-section from ALO1 to ALO2.

2.2. Completion details of the Boreholes

A total of ten boreholes were drilled at specific locations within and just outside the fenced landfill. The whole landfill area is shown in Figure 3 above, and consists of the old landfill and a newer landfill area. The waste dumped in these landfills contains metals that have dissolved into the groundwater.

The majority of boreholes are situated on a landfill that is currently in use. However, the MLSO1 and SW2 boreholes are located in a region of an old landfill that is believed to have very high pollutant concentrations in the groundwater, approximately 6-8m below the surface. This conclusion has been drawn from the data collected from the site prior to the 9th May 2002. ALO1 is situated just outside of this old landfill zone.

There are five all-level (AL) observation boreholes that are not eligible for extracting water samples because the water from all depths in the profile mixes together. There are three multi-level sampling (MLS) boreholes, which consist of nylon tubing cut to various lengths and these boreholes provide access to the groundwater at known depths. Details about the finishing of the MLS boreholes and the AL boreholes can be found in Appendix 1 and Appendix 2, respectively.

2.3. Previous research at the site

Initial research has been carried out at the site. It has broadly tackled the geological setting, the geophysical properties of the landfill area, the change in water table heights with time and the geochemical properties of the groundwater.

Soil samples were collected from the site during the drilling process and these have been analyzed using Aqua Regia Digest, scanning electron microscopy (SEM) and X-Ray Diffraction (XRD) (Klug, 1954) to determine the ratios of different soil constituents. Sand was the major constituent and clay was found in very small amounts.

Automatic logging techniques and one-day pressure head measurements in the boreholes have been used to gather data about the water heads on the landfill site. There are daily changes in the head heights in the boreholes related to the influx of seawater at high tide and then the ebbing effect at low tide. The magnitude of this effect decreases with the distance away from the estuary (refer to Appendix 3).

Logging methods were used to collect temperature, electrical conductivity and pH data from BH4 and SW2. The temperature data shows a gradual decline in values through November to March (refer to Appendix 3). This could be due to the warmer water temperatures during the wintertime caused by the high specific latent heat of water. Electrical conductivity was monitored in BH4 and SW2 but there did not appear to be any long-term changes in SW2. There were more variations in BH4 but there did not appear to be visible cycles occurring.

Groundwater sampling and analysis has been carried out in the MLS boreholes. The samples were analyzed using ICP-AES analysis and trends were noticed. The concentrations of some elements in the water were found to be lower at high tide than at low tide. This could demonstrate that the changes in the hydraulic gradients of the water table could affect the movement of elements. The concentration profiles in each MLS borehole show a large concentration of specific elements that are found in the landfill, e.g. zinc, aluminium, manganese etc., in the uppermost few metres and then concentrations decrease with depth. MLSO2 has been found to have higher concentrations of zinc than MLSO1 or MLSO3 and this is thought to be the location of a pollutant plume. The monitoring of the groundwater chemistry will determine whether this plume is moving at any significant rate. Figure 7 shows the approximate position of the plume. The AL01 borehole cannot be used to obtain water samples but it was noticed during the drilling process, and later during the monitoring of the borehole, that an organic pollutant is present in the water. It is obvious by a dark slime that covers the probes and their cables.

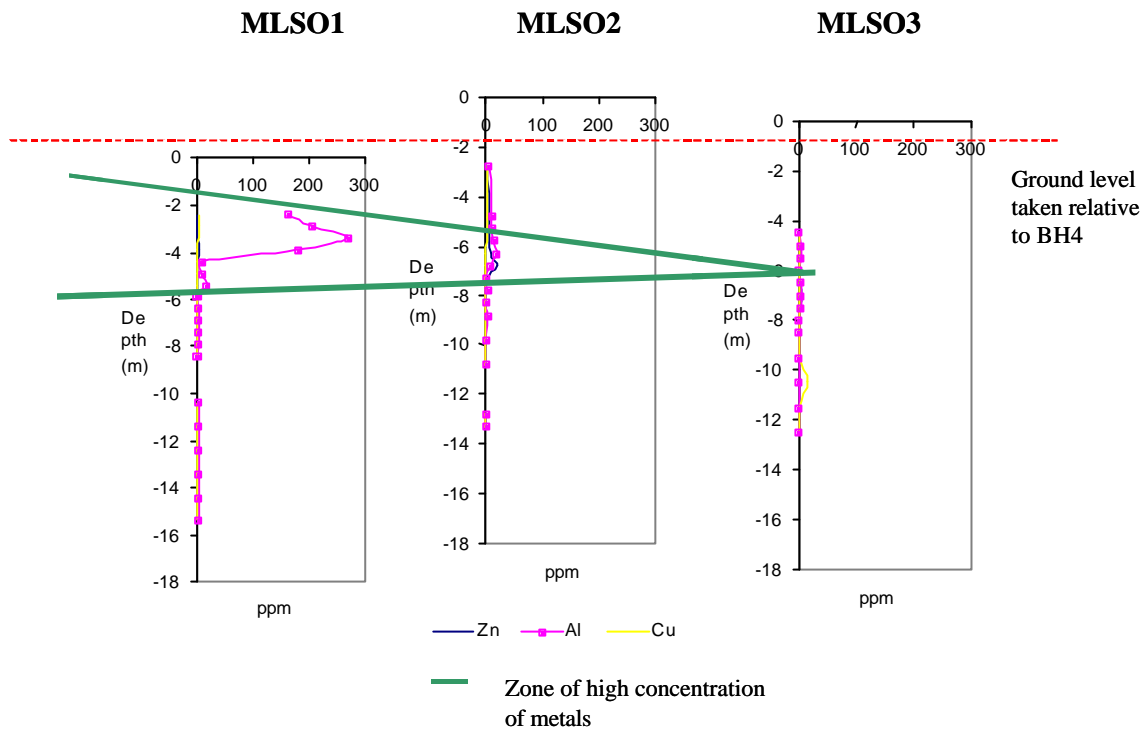


Figure 7: The current approximate location of a leachate pollutant plume. The borehole heights have been corrected to ground level at BH4.

2.4. Aims

Several aims were covered:-

- To determine an average hydraulic conductivity of the formation by carrying out a slug test in ALO3 to induce a water displacement in the borehole. The change in pressure was monitored over time. This data was configured and analyzed using the Hvorslev method.
- To produce a cross-section of the site from ALO1 to the estuary using the geological profiles of the boreholes.
- To analyze the spatial and temporal variations that may occur in the metal concentrations in each borehole throughout a three-week sampling period. Water samples were taken from the MLSO1, MLSO2 and MLSO3 boreholes (shown in Figure 3) on the 05/06/02, 13/06/02 and 20/06/02 and analyzed for zinc and sodium. Zinc was used as an indicator of a leachate pollution plume and sodium was used to indicate the height of the saline influence from the sea. The data on the zinc concentrations were analyzed to demarcate the extent of a pollution plume in the groundwater.

- To determine if any periodic cycles can be witnessed in the water chemistry during the tidal cycles in the estuary by comparing the water chemistry data from the boreholes to the dates and times of spring and neap and high and low tides. Old data suggests that there is a relationship between the stage of the cycle (spring or neap tide) and the concentration of elements witnessed in the MLS boreholes.
- To determine whether there is evidence for the presence of a pollution plume by measuring the pH and electrical conductivity of the water samples when extracted from the coastal aquifer.
- To determine the effect of seawater intrusion on the gradient of the water table and determine the groundwater flow direction, using head data. The head in all of the boreholes was measured on each day that groundwater samples were taken using a dipper.
- To determine whether there are long term variations in the pH, temperature and electrical conductivity values by data logging in borehole ALO3. A 3-week period of continuously logged data on electrical conductivity, pH and temperature at fixed locations in the borehole was collected. This will provide data to reinforce the information gathered from the water samples in the MLS boreholes.

There is still research actively undertaken to establish the hydrological and hydrochemical characteristics of the Ardeer site. This investigation was carried out as a collaboration of skills from Edinburgh and Lancaster Universities and the project is being funded by the Leverhume Trust.

3. Method

3.1. In-situ Monitoring

3.1.1. Head Measurements

The head in the boreholes was measured during the sampling period on the site. A dipper was used and the depth to the water table was measured off the calibrated tape. All the measurements were taken to the top of the outer casing and compared to BH4 to determine the depth from a single datum. BH4 was used as this reference datum. The head readings were then used to determine the approximate water table gradients in order to determine the groundwater flow direction.

3.1.2. Slug-testing in ALO3

Slug testing was carried out on the 9th of May 2002 in ALO3. A pressure transducer was placed in the borehole at the initial depth of the water table and this depth was recorded. A sand-filled slug was dropped into the well to induce an instantaneous increase in the head. This initiated a falling head test and the pressure transducer recorded the decrease in head pressure every four seconds. Three slug tests were carried out successfully; one falling head test and two rising head tests were carried out. This data was then used to calculate the hydraulic conductivity of the aquifer around the borehole.

3.1.3. Vertical Chemical Profiles in ALO3

The vertical profile of pH was roughly determined using a pH probe and lowering it slowly down the borehole, starting at the top of the water table. The reading of the pH was taken every 4 seconds and the lowering of the probe was at a rough speed of 1m/s. The probe was lowered to a depth of 13.04m.

An electrical conductivity profile was developed for the ALO3 borehole by lowering the probe from the top of the water table, 3m. The reading of the conductivity occurred every 4 seconds and lowering speed was roughly 1m/s.

3.1.4. Continuous data logging of Temperature, pH and Electrical Conductivity in ALO3

A logging setup was created in the ALO3 borehole to log the temperature, pH and the electrical conductivity. A temperature probe was connected to a power supply and data logger unit and placed in the borehole at a depth of 4.2m. A pH probe was set up to log at a depth of 4m.

Three probes were used to log the electrical conductivity at depths of 3.7m, 4.5m and 6m. The electrical conductivity was monitored at three depths to compare the profile with the vertical changes seen and to monitor temporal changes in the conductivity over time.

All the probes were below the average range of head change in ALO3 so they would constantly be submerged.

3.2. Groundwater and Surface water Sampling

Chemical sampling was carried out weekly over a three-week period starting on the 5th of June. Monitoring of the pH, electrical conductivity and temperature in borehole ALO3 occurred over a six-week period starting from the 9th of May.

3.2.1. Multilevel sampling boreholes (MLS)

There are three MLS boreholes (refer to Figure 3). These boreholes are appropriate to use to obtain water samples because they provide a relatively undisturbed sample at a specific depth whereas the water in the other boreholes mixes from all depths. The boreholes were sampled on the 5th of June, 13th of June and 20th of June.

Water samples were taken, using a new plastic 50-60ml disposable syringe, and collected in a 100ml plastic beaker. The temperature and electrical conductivity were measured and recorded. Then the samples were split into two separate 50ml Nalgene bottles and these were labeled stored, awaiting filtration. The full sampling method can be found in Appendix 4.

3.2.2. Estuarine Sampling

Some sampling was carried out in the estuary. There is no current monitoring carried out of the estuarine water and so samples were taken to compare sodium and zinc concentrations in the seawater to those sampled in the groundwater. This could be useful to assess the effect of the tides on the metal concentrations in the groundwater.

The height of the water in the estuary is affected by the stage at which the tide is along the tidal cycle. Sampling was carried out as the tide was ebbing and so the water level was not at its maximum height. The tidal influence in the estuary is 5 meters in a spring tide.

Three samples were taken from the estuary and they are shown in Figure 8:-

- Sample 1 – In a parallel line with the MLSO3 borehole.
- Sample 2 – In a parallel line with BH4.
- Sample 3 – In a parallel line halfway between BH4 and the MLSO3 borehole.

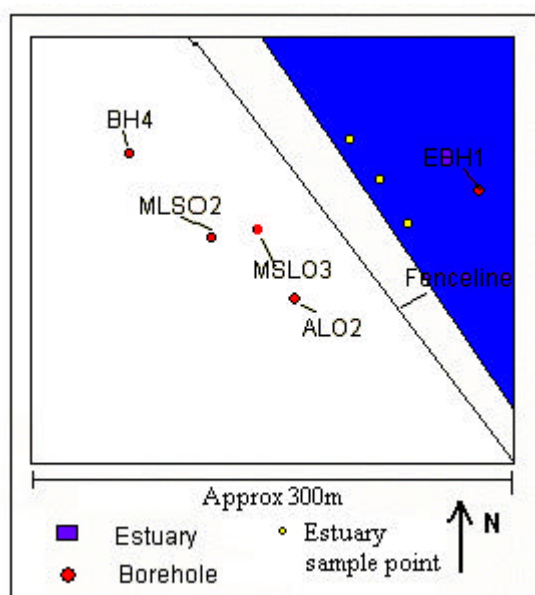


Figure 8: Sketch map of the locations of the estuarine sampling sites

The sampling was carried out by standing downstream of the sampled water, or as far away from the sampled water as possible, to avoid any contamination. Measures were taken to avoid stirring up the sediment and reducing the amount not naturally found in the sample. Samples were taken approximately two meters from the edge of the water and the Nalgene bottles were rinsed in the water downstream beforehand.

3.2.3. Filtration of groundwater samples

Filtration of the samples occurred in the ICI laboratories at Ardeer. Two filtering suction systems were used to increase the filtering speed of all the samples. The samples were tipped through a porcelain filter unit containing a Whatman 40 paper filter sheet. The filtered sample was separated into the original Nalgene bottles, after rinsing with deionised water. Two drops of hydrochloric acid were added to the bottles to prevent any dissolved metals from precipitating out of solution. For a more detailed method refer to Appendix 4.

3.4. Atomic Absorption Spectroscopy

As defined by Ramirez-Munoz (1968), atomic absorption spectroscopy is

“An instrumental spectro-analytical method which is based on the measurement of the absorption produced in a beam of radiation of suitable wavelength proceeding from an emitting source of constant intensity, by a medium composed of atoms of the element to be determined”.

A liquid sample is sprayed into a nitrous oxide-acetylene flame and the solution is atomized. This does not affect the energy of the atoms and they are still at ground state. A beam of light, of specific wavelength corresponding to the analyte to be analyzed and of a known intensity, is emitted from an appropriate source and sent through the flame. Each element absorbs a specific amount of energy in order to become excited and only the required analyte will absorb the energy at this wavelength. The emitted amount of light from the source is known and therefore the amount of light absorbed by the atoms can be used to work out a total absorbance.

The absorbance increases with the concentration of the analyte in the sample and so the concentration can be worked out by comparing absorbance to a calibration graph, determined by the analysis of prepared standards.

3.4.1. Advantages

1. The experimental procedure is very simple and training and supervision is minimal. The time for analysis is very short and so length of time in the laboratory is shortened. There is a relatively low price involved when cost per analysis is calculated.
2. The technique is very versatile and takes a small amount of time to switch between elements.
3. There are fewer inter-element interactions and the method allows for greater sensitivity. Certain elements are not easily analyzed using emission methods.
4. Absorption is less dependant on the temperature of the flame (Ramirez-Munoz, 1968) because only the atoms in the ground state are utilized. However, there may be chemical interferences (certain compounds) that prevent the formation of a vapour.
5. The method has good repeatability and so good results are produced. The machine is accurate and precise. This all depends on the age of the equipment and maintenance of the components of the system i.e. the lamps, the quality of the flame, the detection system etc.

3.4.2. Disadvantages

1. Precision may vary between various elements and this is associated with the emitting source and the flame. An unstable lamp also creates a lot of noise. The price of lamps can be a drawback for large laboratories that do analysis on many different elements.

2. It is more difficult to produce ground-state atoms for some elements than others, such as aluminium, molybdenum, silicon, tungsten and titanium. This can be overcome by using fuel-rich flames.
3. Some solvents can cause some absorption of the emitted light that affects the accuracy of the concentration value that is determined for the sample.
4. There is less flexibility for varying sensitivity to analyze a sample over a wide range of concentration and so dilutions need to be made.

3.4.3. Analytical Technique

A zinc standard solution of 100ppm Zn was diluted to a 10ppm concentration using deionised water. This 10ppm standard was then used to create six analytical standards ranging from 0ppm to 1ppm in appropriately labeled 100ml volumetric flasks. The standards were analyzed using the spectrometer and the results and standard deviations were recorded. The results were used to create a calibration graph of concentration against absorbance.

The samples were analyzed on the spectrometer straight from the Nalgene bottles and any dilutions that were necessary were made and recorded. The final concentrations of zinc in the samples were found by using the calibration graph. A detailed method can be found in Appendix 5.

3.5. Flame Emission Spectroscopy

This involves the use of a liquid sample that is also sprayed through a nitrous oxide-acetylene flame. However, in this method the flame is used to atomize and provide the energy necessary to excite the atoms in the vapour. An atom will always revert back to ground state and therefore will emit an amount of energy equal to the amount needed to excite it. This amount is specific to each element and therefore the amount of emitted radiation of the appropriate wavelength is recorded through a slit. The emitted radiation travels in all directions but enough passes through the slit to gain an accurate measure of the concentration of the analyte in the sample.

The amount of emitted radiation increases with the concentration of the analyte in the vapour. Therefore the concentration of the analyte in a sample can be determined by comparison to a calibration graph, produced using prepared standard solutions.

3.5.1. Advantages

1. This technique offers a better degree of sensitivity when analyzing alkali metals.
2. It is much easier to carry out multi-component analysis with a single source by setting selected radiation corresponding to each analyte.
3. The machine can be rapidly switched between testing for various elements. Do not need to change emitting source.
4. Cheap and relatively simple analytical method. Users need little supervision or training for basic usage.

3.5.2. Disadvantages

1. The precision is limited by the stability of the flame.

3.5.3. Analytical Technique

A sodium standard of 1000ppm was diluted down to a 100ppm standard. This was then used to create a range of 5 standards from 0-4ppm in appropriately labeled 100ml volumetric flasks. These standards were then used to calibrate the machine emittance dial. The dial was set to 0 for 0ppm and 100 for 4ppm.

The samples were run through the machine and more dilutions were necessary, due to high levels of background sodium concentrations. Therefore, dilutions were done at the machine using pipettes and smaller volumes of sample to save time. The final sodium concentrations in the samples were found by referring to the calibration graph. This concentration was then multiplied by the inverse of the dilution factor to gain the total initial concentration. A detailed method can be found in Appendix 5.

In summary, measurements were carried out in the boreholes to collect height data of the water table and then in-situ measurements on pH, electrical conductivity and hydraulic conductivity. These were carried out as vertical cross-sections in AL03 using probes, by use of a slug test using a pressure transducer or at specific depths over time. Temperature was also logged at a specific depth with time using a probe.

Groundwater sampling was carried out in the multi-level sampling boreholes and samples were contained in plastic Nalgene bottles after the pH and electrical conductivity had been measured. Surface water sampling was carried out in the estuary and samples were stored in plastic Nalgene bottles. All the samples were filtered in the Ardeer laboratories.

Atomic absorption spectroscopy and emission flame spectroscopy were used to analyse the water samples for zinc and sodium concentrations respectively. The concentrations were then plotted as vertical borehole profiles.

4. Results

4.1.1 Fluctuations in the water table

Head measurements were gathered for the 9th of May and the 5th of June. These were corrected with respect to the ground level at BH4. The values are shown in Table 1.

Table 1: Head measurements in the boreholes on the 9th of May and the 5th of June.

Date	ALO1	ALO2	ALO3	BH4	SW2
09/05/02	2.218	2.829	2.654	2.725	2.386
05/06/02	2.293	2.864	2.724	2.805	2.481

The two dates that the heads were measured on were both on a Neap tide, however the sampling times varied by two hours and the time that the high and low tides occurred varied by three hours, so there is an average difference between the two sampling times of five hours. Therefore, the two sampled dates are at different tidal heights, the 9th of May being measured at a high tide and the 5th of June was sampled at a low tide. The distances between the boreholes, shown in Table 2, were calculated using the x and y coordinates of a pre-existing coordinate system designed at the beginning of the monitoring project. The coordinates and the details required to correct measurements for BH4 can be found in Appendix 6.

Table 2: The horizontal distances between the boreholes

	ALO1	ALO2	ALO3	BH4	SW2	MLSO1	MLSO2	MLSO3
ALO1	0	126.894	111.036	77.411	45.43	51.019	92.011	110.054
ALO2	126.894	0	33.158	71.857	82.752	59.134	36.956	23.46
ALO3	111.036	33.158	0	77.947	65.718	29.526	40.783	42.229
BH4	77.411	71.857	77.947	0	52.792	59.134	38.024	48.675
SW2	45.43	82.752	65.718	52.792	0	5.59	50.552	68.677
MLSO1	51.019	77.4	29.526	59.134	5.59	0	45.922	63.921
MLSO2	92.011	36.956	40.783	38.024	50.552	45.922	0	18.222
MLSO3	110.054	23.46	42.229	48.675	68.677	63.921	18.222	0

The head measurements were then used to determine the direction of flow in the aquifer, which is shown by Figure 9. This was produced assuming that the differences in the corrected heads would cause flow to occur from areas of higher head to areas of a lower head. However, this may not be the case because it appears that water flows towards a point from where it appears also to be flowing towards that point, shown by water flowing from ALO1 to ALO2 but from ALO2 towards BH4. Water flow direction is towards the ALO2 borehole and therefore towards the sea when the tide is high.

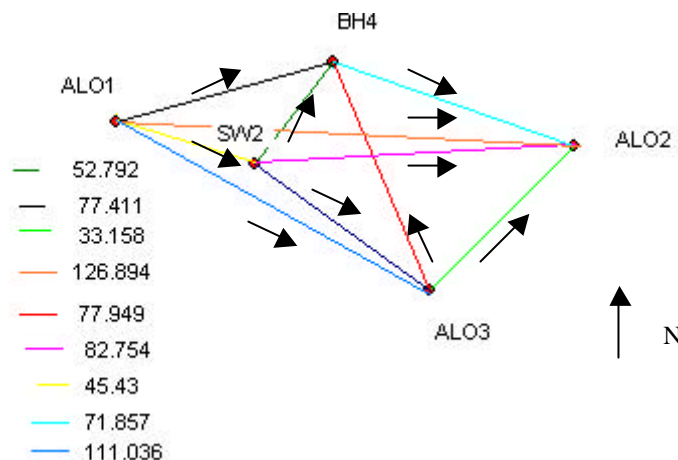


Figure 9: The approximate flow directions shown using the assumption that water will flow to the lowest levels. This is for the 9th of May, 2002. All the measurements are in metres.

The diagram was much the same for the measurements carried out on the 5th of June, except that the hydraulic gradients between the boreholes were greater, meaning that the flow towards the sea was faster.

4.1.2 Hydraulic conductivity of the aquifer

The static water level in a borehole is the water level of the undisturbed aquifer before the slug has been injected or removed. Three tests were carried out, two rising head tests and one falling head test. The static water levels for each test were taken as the water level prior to the following test as there appeared to be an initially very rapid response followed by a much slower response in the rising water levels before they could return to the water levels prior to the slug testing. The methods used to prepare the data were taken from Fetter (2001) and Butler (1998).

The slug test data was processed to produce a plot of the ratio of h/h_0 against time. This is shown for the three slug tests in Figure 10, 11 and 12. A trend line was fitted to each dataset to obtain an equation for that line.

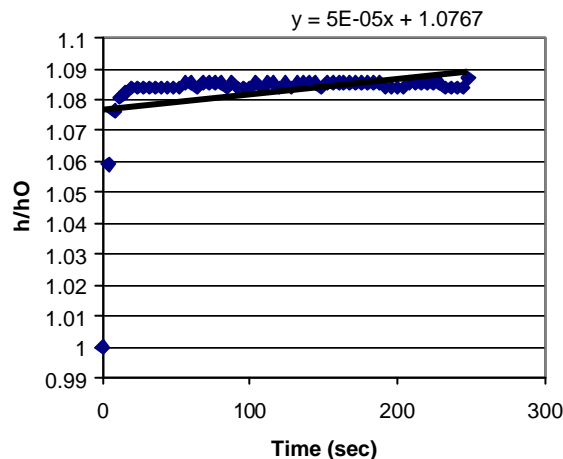


Figure 10: The plot of h/h_0 against time for the first rising test in ALO3.

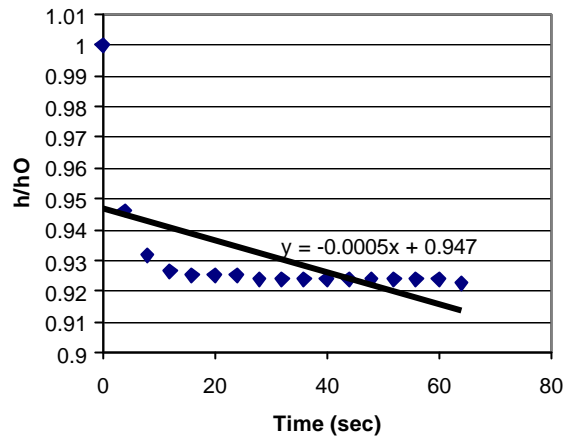


Figure 11: The plot of h/h0 against time for the falling test in ALO3.

The hydraulic conductivity (K) was calculated using the equation

$$K = \frac{r^2 \ln(L_e/R)}{2L_e t_{37}} \quad (1)$$

where

K is the hydraulic conductivity (cm/s)

R is the radius of the well screen (20cm)

r is the radius of the well casing (5cm)

L_e is the length of the well screen (900cm)

t_{37} is the time it takes for the water level to rise or fall to 37% of the initial change (s)

(Fetter, 2001). This is the general formula developed by Hvorslev to determine the hydraulic conductivity when using data from piezometers that do not fully penetrate an aquifer.

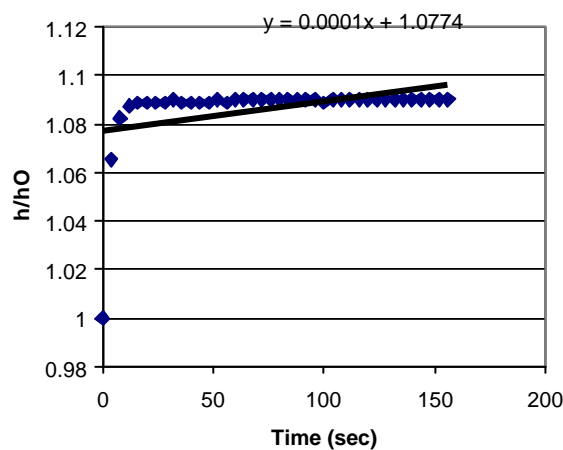


Figure 12: The plot of h/h0 against time for the second rising test in ALO3.

The values of K are very similar and are shown in Table 3.

Table 3: Hydraulic conductivity estimated using the Hvorslev method.

Slug Test	Hydraulic conductivity (m/day)
Rising Head 1	42.4
Falling Head	48.4
Rising Head 2	42.4

4.2 Geochemical variations in the aquifer

4.2.1 AL03 Borehole

4.2.1.1 Vertical Chemical Profile

The vertical profiles for the pH and electrical conductivity in borehole ALO3 can be seen in Figure 11.

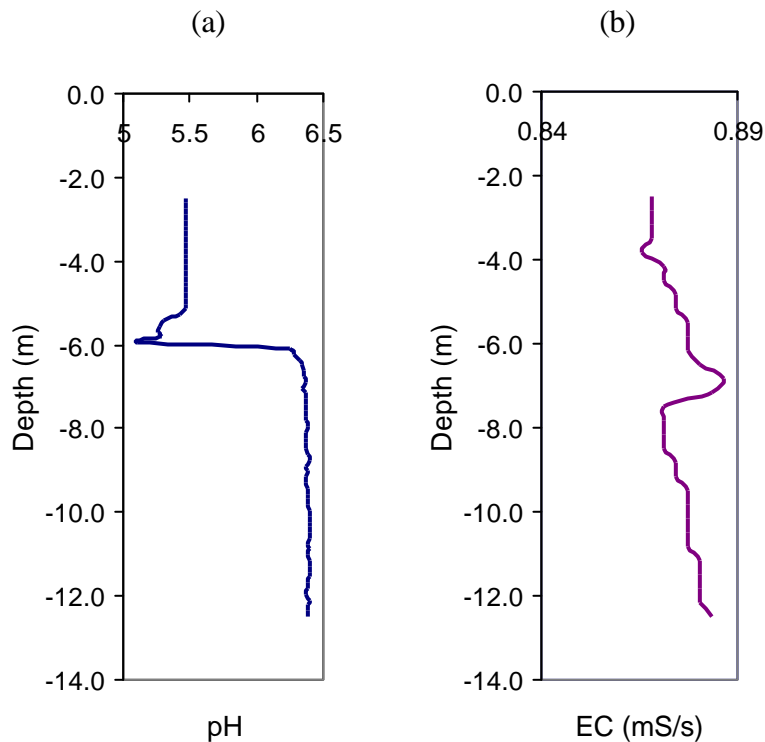


Figure 13: Plots of the vertical profiles of the parameters pH and electrical conductivity in ALO3. Data collected on the 9th of May, 2002.

It is shown in Figure 13 that there is marked change in the pH of the groundwater at a depth of 6m. The pH of the water above a depth of 5.5m is 5.5 but this decreases to a value of 5 at a depth of 6m. Between 6 and 6.5m depth in the profile there appears to be a

strong buffering force acting and there is an increase in pH of a whole unit. The pH becomes almost constant with increasing depth and assumes a value of 6.3 at a 12m depth.

The conductivity value will indicate the ability of the groundwater to pass a current of electricity. This can usually be increased with an increase in the amount of ions in solution. There is an overall increasing trend of the conductivity with depth. There is a peak in the conductivity at a depth of 7m.

4.2.1.2 Monitoring of electrical conductivity, temperature and pH

The electrical conductivity was logged from the 9th of May until the 20th of June. Over this period two depths were monitored, 4.5m and 6m. The data collected is shown in Figure 14 and 15. At the start of logging, shown in Figure 14, the conductivity increased at both depths by 0.01mS/cm. Then a plateau value of 0.87mS/cm was reached at a depth of 4.5m, which was maintained over 2 days. The conductivity then increased by a further 0.01mS/cm to a new plateau value, up to the 23rd of May. There were decreasing fluctuations in the EC value during this period. After the 23rd of May, the conductivity decreased again to 0.87mS/cm. After the initial increase in conductivity at 6m the plateau value of 0.77mS/cm was reached. This was maintained for most of the time period shown in Figure 14. There were two short periods where the conductivity increased by 0.01mS/cm, which were the 18-19th of May and the 22nd of May. On the 24th of May the conductivity at 6m dropped by 0.02mS/cm and this was maintained for 2 days, thereafter increasing by 0.01mS/cm. This then decreased again on the 28th of May. The two patterns are similar but there appears to be larger short-term changes experienced at 4.5m.

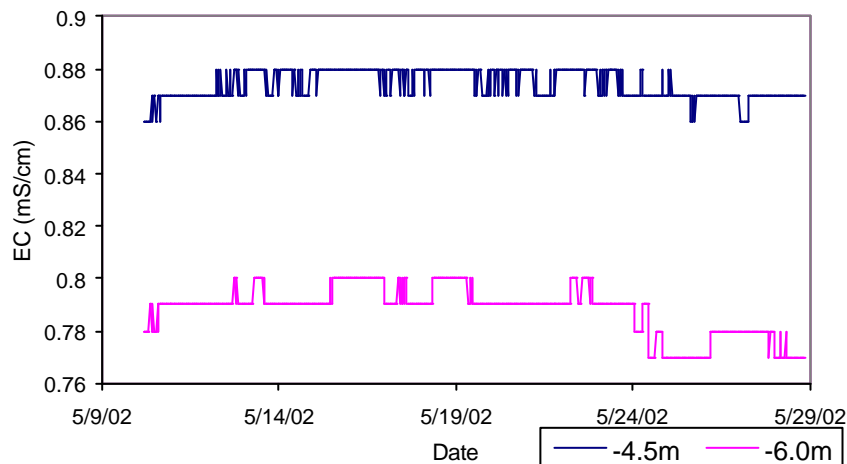


Figure 14: The temporal changes shown in the electrical conductivity that was logged at depths of 4.5m and 6m from the 10th of May to the 28th of May.

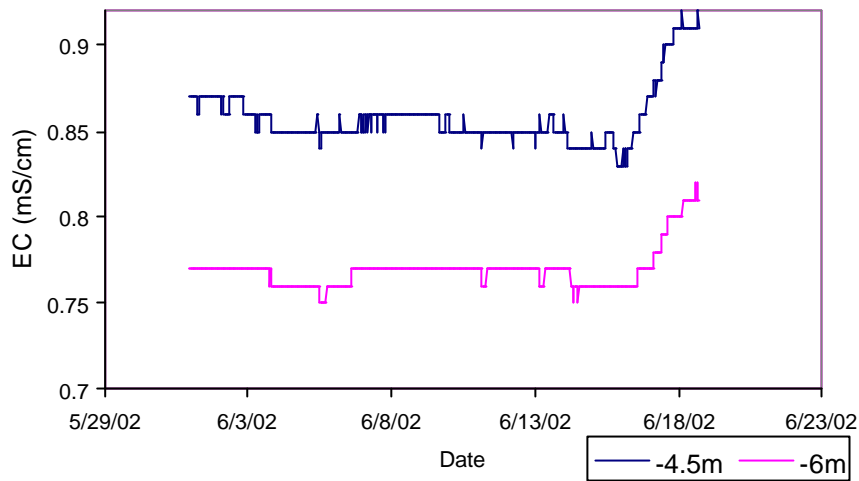


Figure 15: The temporal changes shown in the electrical conductivity that was logged at depths of 4.5 and 6m from the 31st of May to the 18th of June.

The temperature of the groundwater was monitored at a depth of 4.2m and the data is shown in Figure 16. There was an average overall increase in the groundwater temperature over the monitoring period of 0.4 degrees Celsius. There are very short-term fluctuations in the temperature that occur throughout the monitoring session but there are two periods where the temperature fluctuations are greater than normal.

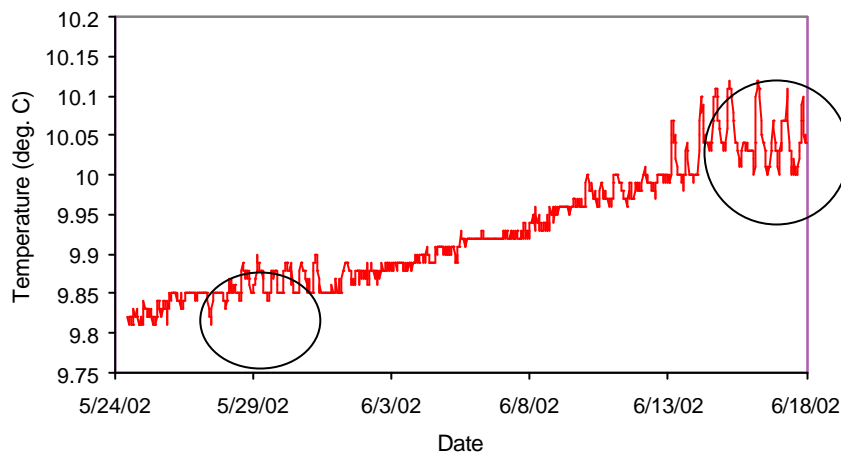


Figure 16: The temporal changes in the temperature of the groundwater monitored at a depth of 4.2m from the 24th of May to the 6th of June.

The monitoring of the pH was done at a depth of 4m and the time series that has been plotted in Figures 17 and 18 correspond to those plotted in Figures 14 and 15. Figure 17 shows that at the start of the time series the pH of the groundwater increases slightly until the 13th of May and this is reflected in the conductivity of the borehole. The overall trend in the pH from the 13th of May until the 28th of May is a decrease in pH of 0.04 pH units.

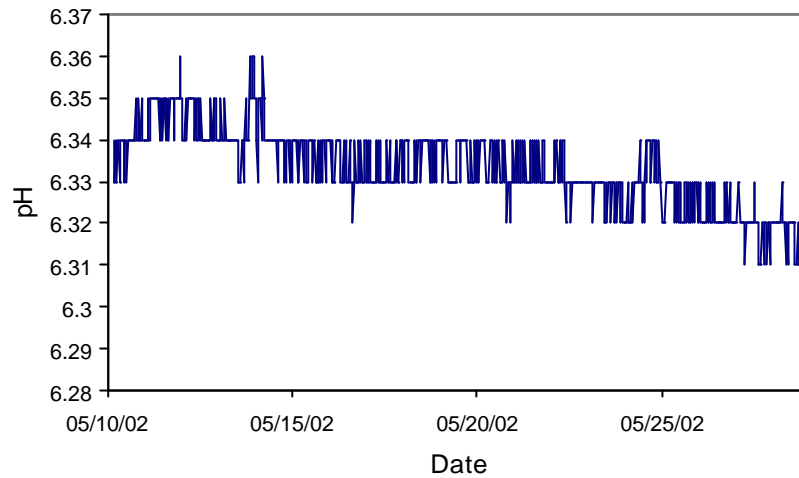


Figure 17: The temporal changes in the pH of the groundwater from the 10th of May to the 28th of May.

From the 31st of May there appears to be an oscillation in the pH from 6.33 to 6.32, occasionally dropping to 6.31. The pH then increases on the 10th of June to a value of 6.35. This higher pH is maintained for 3 days or so and then the pH starts to decrease to the lowest pH values, 6.29, witnessed during the monitoring period.

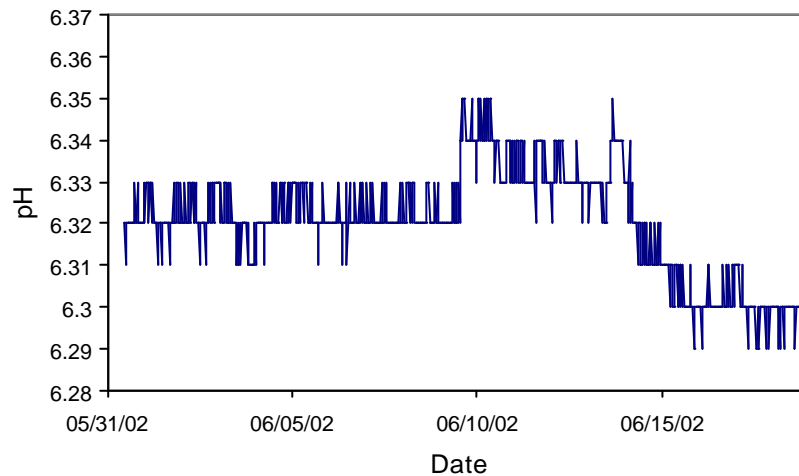


Figure 18: The temporal changes in the pH of the groundwater from the 31st of May to the 18th of June.

Over a period of two to three days there is a pattern where the pH increases and decreases by 0.01 pH units. This is shown in more detail in Figure 19.

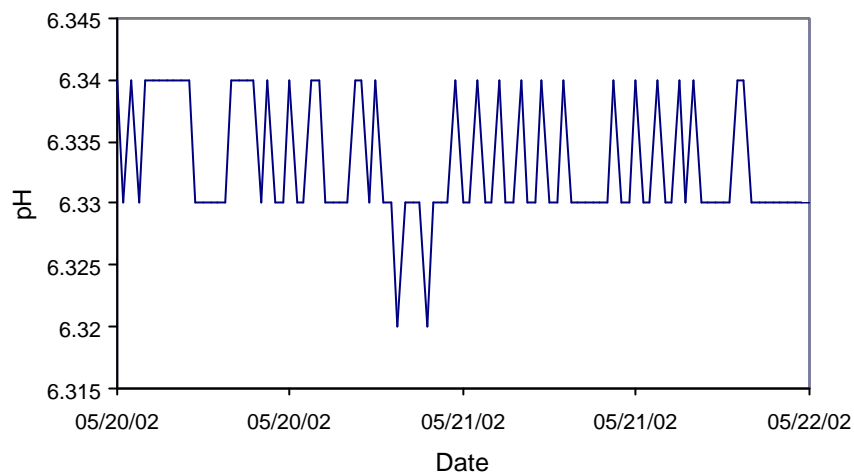


Figure 19: The short-term pH fluctuations in the borehole over a 2-day period

4.2.3 MLS Boreholes

4.2.3.1 Daily spatial variations

The three boreholes were monitored on each day for their zinc and sodium concentrations and also their pH and conductivity values.

Firstly, with regard to the zinc concentrations in the boreholes, the highest concentrations are found in borehole MLSO2 on all the sampling dates. This can be seen in Figure 20. All the peaks in concentration that are found correspond to similar depths in the borehole, the highest concentrations are found between 4 and 8m. On the 5th of June, there are two peaks in the zinc concentration in MLSO1, which are found at 4.4m and 6m depths. There is one main peak in MLSO2 with a very slight second peak and these are at 5.5 and 6.5m depths. There are three peaks witnessed at MLSO3 and these are found at the start of sampling at 4.3m then 6m and 7m depths. This pattern is repeated on the 13th of June but varies slightly on the 20th of June. It appears that the concentration of zinc in MLSO2 has increased and has similar levels as MLSO3. This can be better seen in Section 4.3.3.2.

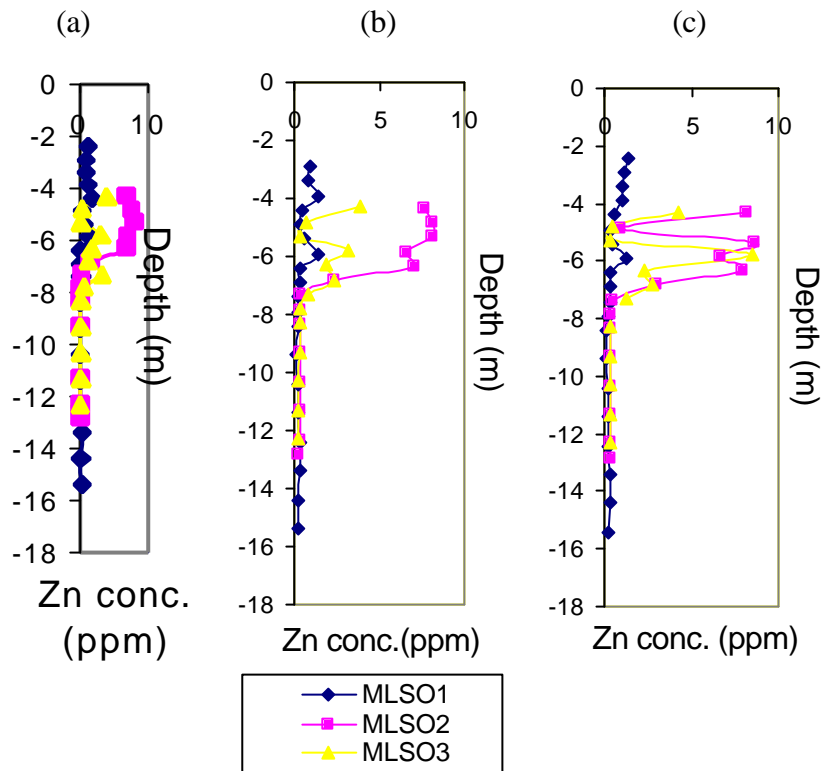


Figure 20: Variations in the zinc concentrations between the MLS boreholes on the three separate sampling dates (a) 05/06/02, (b) 13/06/02 and (c) 20/06/02

With regard to the sodium concentrations in the boreholes, the general pattern is that the concentration of sodium increases with depth in the boreholes. This is true for MLSO1 and MLSO2 but there is also a high concentration of sodium found at a depth of 5 meters in MLSO3.

MLSO2 and MLSO3 are not deep enough to witness the extent of the increase in sodium concentration at depth. It can be extrapolated from the data that is there that the sodium profile for these boreholes may look similar to MLSO1.

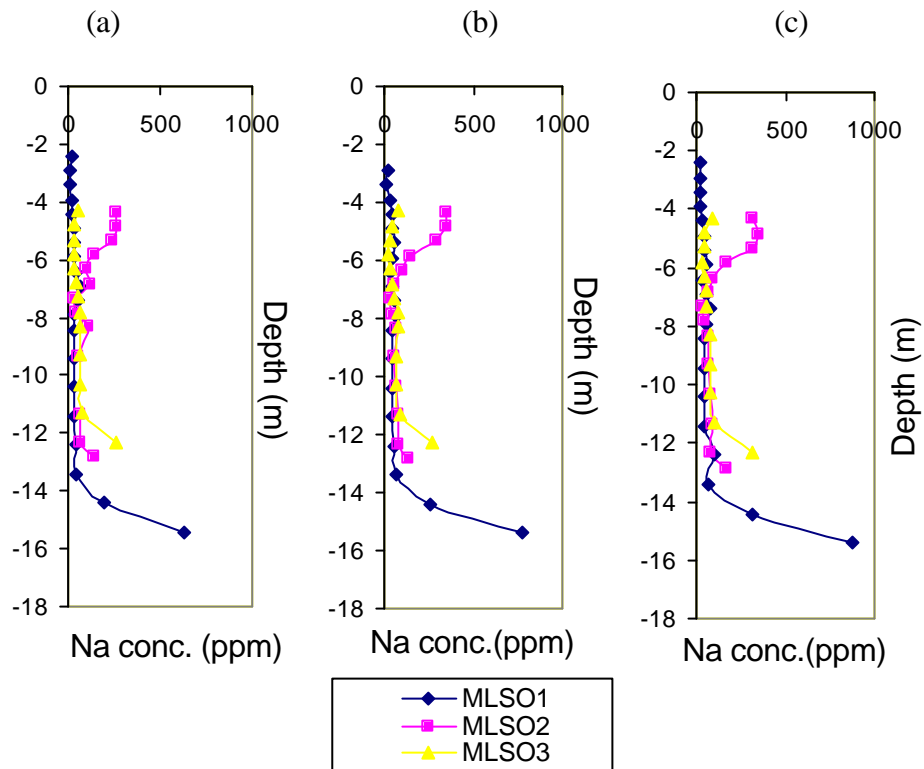


Figure 21: Variations in the sodium concentrations in the MLS boreholes on the three separate sampling dates. (a) 05/06/02, (b) 13/06/02 and (c) 20/06/02.

Figure 22 shows the data found when monitoring the electrical conductivity of the boreholes. The electrical conductivity of the MLSO1 borehole is the lowest of the three boreholes, except between 6 and 8m where there is a peak in the conductivity. The conductivity is high in the upper meters of the boreholes and then decreases. The decrease in conductivity occurs at 4m deep in MLSO1 and between 6 and 8m in MLSO2 and MLSO3.

In the upper meters of the boreholes it is borehole MLSO2 that has the highest electrical conductivity values but the electrical conductivity in MLSO3 becomes the highest of the three boreholes when depth increases.

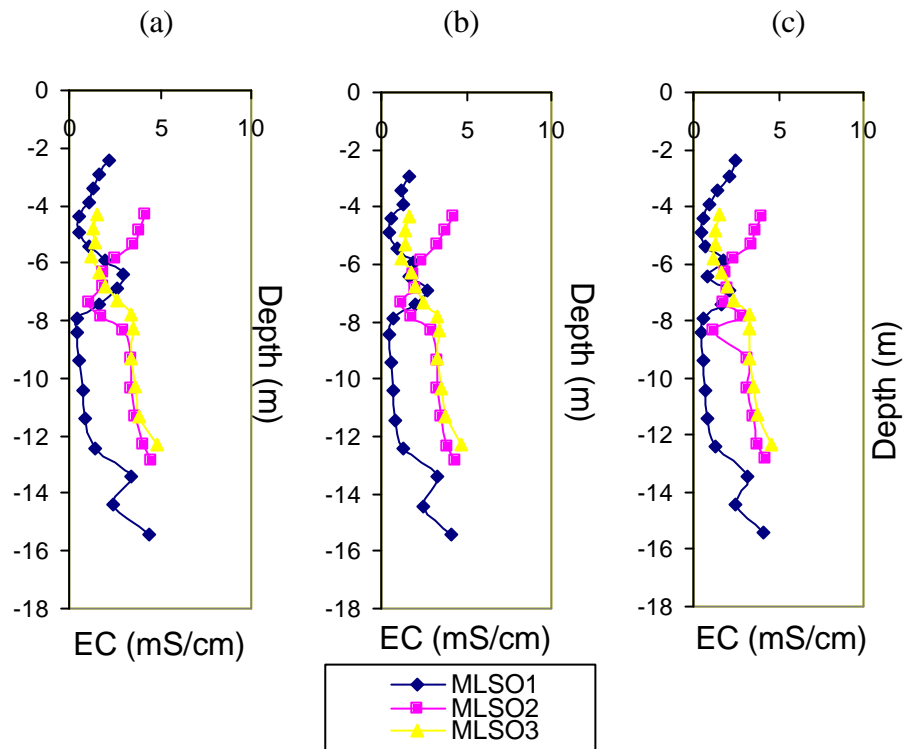


Figure 22: Variations in the electrical conductivity in the MLS boreholes on the three sampling dates. (a) 05/06/02, (b) 13/06/02 and (c) 20/06/02.

The pH is plotted in Figure 23 and it increases with depth, being the lowest in the first few meters. The pH in MLSO1 and MLSO2 are very similar and the boreholes both experience a region of buffering at a depth of 5.5m down to 6m. In MLSO3 the pH is generally more alkaline. There is a region of lower pH 6.5 to 8m depth and some pH buffering occurs at 7m deep. The pH reaches a maximum of 7 at the bottom of the borehole profiles.

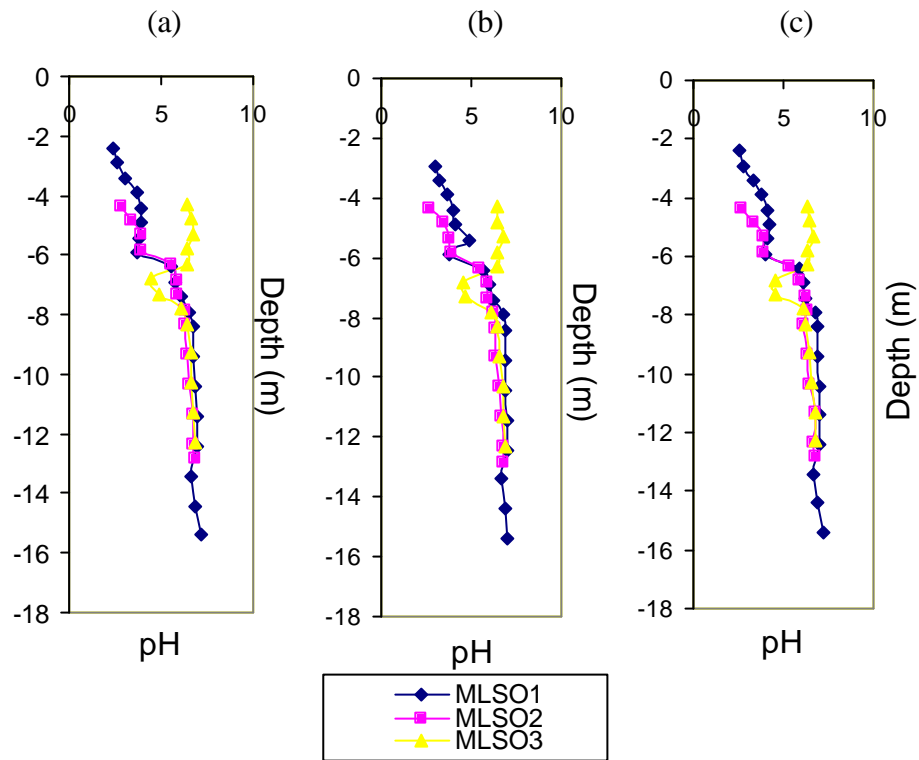


Figure 23: Variations in the pH in the MLS boreholes on the three sampling dates. (a) 05/06/02, (b) 13/06/02 and (c) 20/06/02.

4.2.3.2 Temporal variations

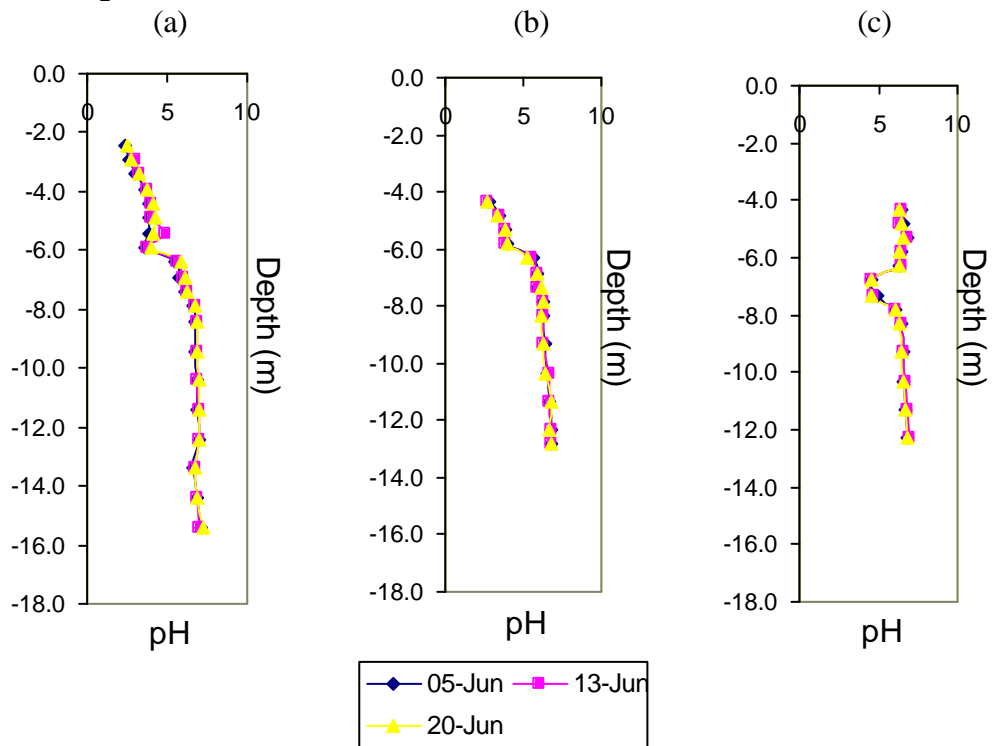


Figure 24: Changes to the pH on different sampling dates in a) MLSO1 b) MLSO2 and c) MLSO3

There is very little variation in the pH of each borehole over the sampling period. MLSO1 has very low pH of 2-4, between depths of 2 and 4m, but the pH is increasing with depth. Then there is a buffering region that occurs between depths of 5 and 6m, where the pH remains constant at approximately 3.7 for a metre in depth. At a depth of 6m the buffering capacity is very low and there is an increase in pH of 1 log unit over a depth of 0.5m. The pH then increases to a maximum pH of 7.

The pH at 4-6m in MLSO2 is very low, ranging from 2-5, but increases with depth. Then the buffering capacity of the soils is very low and the pH increases from 5-6 in 0.5m depth. Then the pH increases to a value of 7.

The pH of the groundwater in the top few metres of the landfill is similar to that at the bottom of the borehole. However at a depth of 7m the pH decreases and is fairly constant for a depth of 0.5m. Then the pH increases to almost the background at 8m. The pH carries on increasing slowly to a maximum of 7.

The electrical conductivity is plotted in Figure 25 and it can be seen that there is little variation in MLSO1, except that it appears that the electrical conductivity profile is shifting down through the borehole profile over time. There is a peak in electrical conductivity at a depth of 6.5m.

The electrical conductivity in MLSO2 on the 5th and the 13th of June are similar with very low conductivity at a depth of 7.5m, but on the 20th of June there are two troughs in the conductivity at depths of 7.4 and 8.4m.

The MLSO3 borehole has very low conductivity at a depth of 4m and then this increases with depth. The patterns in the conductivity are reflected on each sampling date.

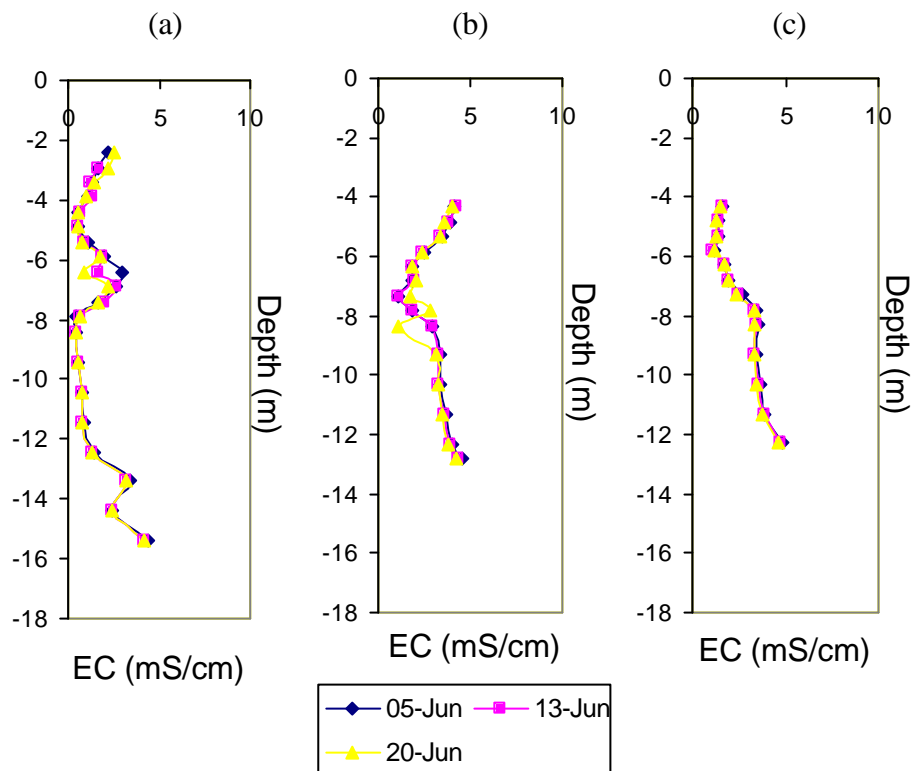


Figure 25: Changes in electrical conductivity in a) MLSO1 b) MLSO2 and c) MLSO3

Borehole MLSO1 experiences two peaks in the zinc concentrations and over time the depths at which the first peak is found, initially at 4.3m, increases.

In borehole MLSO2, there is a high concentration of zinc from depths of 4m to 6.5m and then a rapid decrease in concentration at 7.5m. There is a very drastic trough in the concentration between 4 and 6.5m that was only shown on the 20th of June. This is mirrored by a very drastic peak in MLSO3 on that same date but MLSO1 appears unaffected.

The zinc concentration profile in MLSO3 has three peaks in at depths of 4m, 6m and 7m. Then the concentration of zinc in the groundwater rapidly decreases.

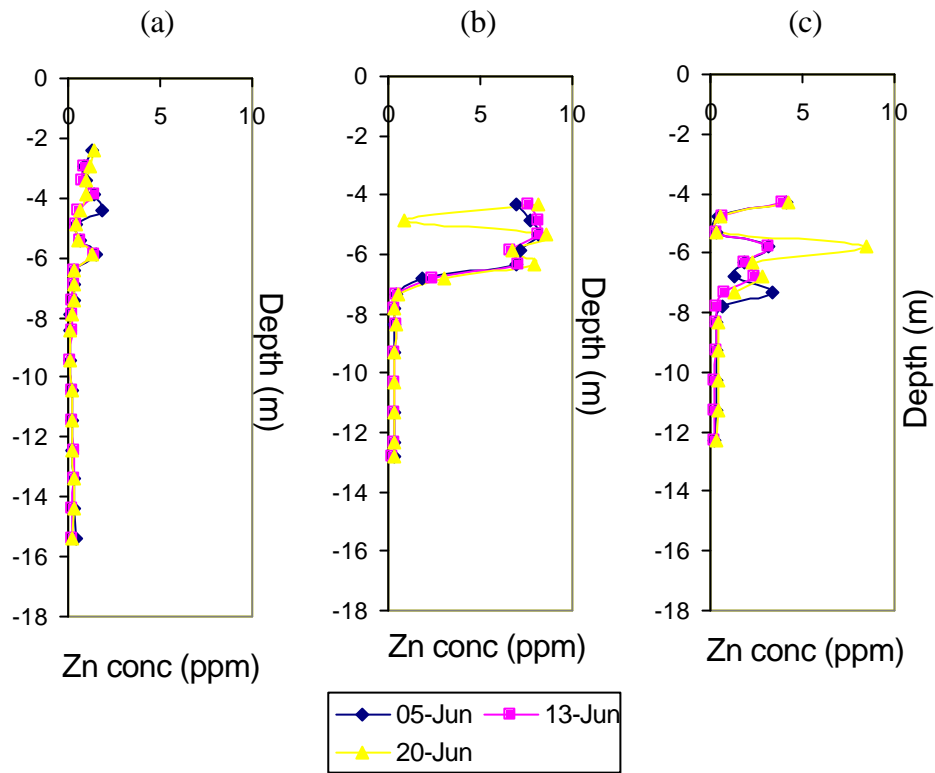


Figure 26: Changes in the concentrations of zinc in (a) MLSO1, (b) MLSO2 and (c) MLSO3.

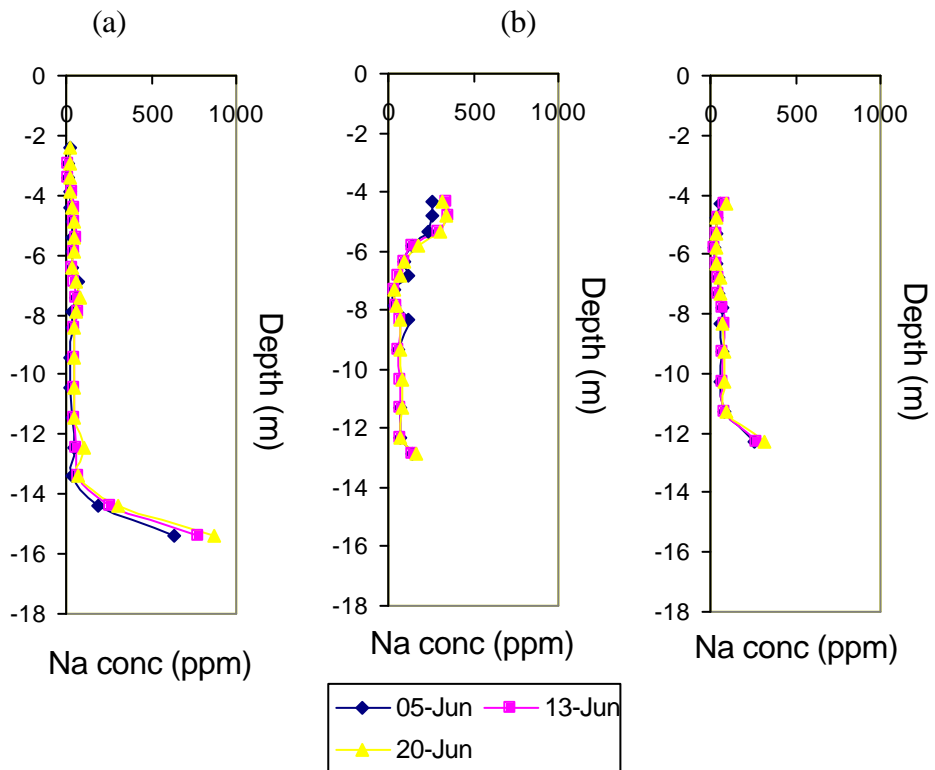


Figure 27: Dataplots of the concentration of sodium in (a) MLSO1, (b) MLSO2 and (c) MLSO3 over the sampling period.

The three boreholes have similar concentration profiles for sodium over the three sampling dates. The concentration of sodium increases with depth in MLSO1 with a small peak in concentration at 7m that levels out to the same previous gradient of increase in concentration. Then at a depth of 13.5m the concentration drastically increases and this continues to the bottom of the borehole.

MLSO2 experiences high concentrations of sodium between 4 and 6m depth and then there is a decrease in concentration to levels similar to MLSO1. There is a small peak in sodium concentration at 8m depth and this then levels out as before. There is then an increase in the concentration again at a depth of 13m. The borehole is not deep enough to determine the full extent of this increase in the concentration.

MLSO3 has a slightly higher concentration of sodium at the top of the borehole but this decreases down to a depth of 8m where the concentration starts to increase again. The increase in concentration becomes more rapid at a depth of 11.8m

5. Discussion

5.1 Hydraulic characteristics of the sandstone aquifer

The two layers of sands and the gravel layer between were assumed to be a single aquifer because the gravel layer acted as an interconnection layer. The boulder clay layer at the bottom of the aquifer was assumed to be an aquiclude and so water moved very slowly in this region when compared to the sands and gravels. The clay layer at a depth of 14m was thus an impermeable layer.

The hydraulic conductivity of the aquifer under the landfill is very high because the material consists of mostly sands and gravels. These have large pore spaces and allow rapid flow of water along a water potential gradient. The value of K will not be constant over the whole aquifer because the geology of the investigated area is very complex. There are lenses of clay that have lower hydraulic conductivities and which may be sites where any pollutants are retained for longer periods of time than in the gravels. The clay is found at MLSO2 at a depth of 5.5m and this may affect the concentrations of the zinc found at this depth. The hydraulic conductivity found for both of the falling head tests were very similar but differed for that of the rising head test. This could be due to the slug actually catching on the pressure transducer that was logging change in the water pressure. It is assumed that the slug is injected instantaneously and that the maximum deviation in pressure occurs straight away. This does not happen because the slug will be affected by the edges of the borehole and there may be blockages in the well screen that prevent the free flow of water.

The boreholes were not fully penetrating and there had also been some decrease to the natural hydraulic conductivity of the materials immediately around the drilled holes. This can cause a value in the hydraulic conductivity that is smaller than should be expected.

The flow directions that were shown in section 4.1.1 show that the flow is predominantly to the estuary from inland and that there is also some flow towards ALO3. However, there is an anomaly in the flow from BH4 to ALO3 because it would be assumed that the

flow would be from BH4 to ALO3 but it is the reverse. This can be explained by either the fact that this flow is found as a result of experimental error because the gradient in this direction is very small, or the shape of the natural land surface of the site, before it was cleared to be used as a landfill, was such that there is a natural drainage path towards ALO3. The landfill is found in an area that was initially sand dune surface and the boreholes could be situated in a natural hollow. The ground surface may have been compacted before the area was filled with ashes and flattened to create the landfill. This could mean that infiltrating precipitation could flow along the compacted original ground surface into the hollow located near ALO3. There is no record of the original ground surface but this theory may be backed by the appearance of a concentration of organic pollutant that only appears to be found at this location.

It was noted that the general flow pattern remains the same at high and low tides, which was not expected. This may indicate that there is more groundwater flow from on land draining towards the sea than the amount of seawater in fluxing the estuary at high tide. The landfill is actually located on a spit-like feature that is affected by the influx of the sea not far away (refer to Figure 2 and the location of the landfill is near the Ardeer factory). Seawater that comes in as high tide is approaching will affect the coastline and this will seep into the groundwater system. This will flow through the aquifer to the estuary, which at this point in the tidal cycle is relatively empty. When the estuary is full at high tide, the influence of the sea on the groundwater at the coastline is much greater than the hydraulic effect of the estuary and so groundwater flows to the estuary but at a slower rate. As the tidewaters ebb away the estuary empties first and then the tidal water leaves the coastline but the groundwater near the estuary still flows toward the estuary because of the hydraulic gradient and the fact that hydraulic conductivity of the aquifer is very high and allows rapid groundwater flow.

The tidal pumping does occur in the estuary but the fluctuations in groundwater levels, that are noticed so vividly during previous head logging of the boreholes on the site, may be caused primarily by the seawater at the nearby coastline rather than be a direct result of the influx of tidal water into the estuary.

The predominant weather conditions will affect the groundwater levels in the aquifer. If there is a large amount of precipitation then due to the high infiltration capacity of the land surface then a lot of water will percolate to the water table. Infiltration is rapid because of the high hydraulic conductivity and therefore the flow direction of the groundwater may be temporarily changed.

5.2 Geochemical interactions

The pH profiles of ALO3 and the MLS boreholes show that there is a very low pH in the top few metres of the landfill. It is reasonable to assume that this is actually due to the production of landfill leachate. This is being produced due to the breakdown of chemical and organic pollutants by various types of bacteria and producing acidic conditions as they anaerobically respire. This high pH is found in the top sand layer of the aquifer because the hydraulic conductivity, even though it is fairly high, is not as high as for the

gravel layer. There is a large amount of groundwater drainage to the sea and therefore when the leachate hits the gravel layer at a depth of 6 to 8m the volume of water that flows through the gravel layer dilutes the leachate and this is where the appearance of a large decrease in the buffering capacity occurs. This could have been explained by the process of cation exchange where the hydrogen ions were sorbed onto the surfaces of particles, however gravels do not have many active sites onto which ions can be exchanged. The pH increases to neutral levels because the drainage of the gravels prevents the contaminated groundwater from traveling further down the borehole profile. The regions where pH buffering occurs, 6.5m in MLSO1 and MLSO2 and 7m in MLSO3, are located just above the gravel layer and may be caused because there is a concentration of landfill material that is releasing just enough hydrogen ions to react with any elements, such as calcium, that cause the natural background pH value of 7.

When the pH was logged continuously it was noted that there appeared to be cycles over a period of a few hours where the pH would range over 0.01pH units. This was very periodic but not constant and so there are processes that may be occurring due to the movement of the draining water through the landfill that are affected by a frequent process. The pH varied over a range from 6.35 to 6.29 and there was an identified increase in pH around the 10th of June. The pH then decreased to lower than before the increase on the 14th of June. This could possibly be related to the fact that this is just after the peak in a spring tide that occurred on the 12th of June.

The electrical conductivity profiles in the boreholes show that there is a high electrical conductivity in the top metres of the borehole where the landfill material is concentrated. This is because as rainfall infiltrates the landfill material it leaches out all the ions that have been released during the biodegradation of the landfill material and so the groundwater here has a high concentration of free ions. The water drains through the profile and as it hits the gravel layer because there is little cation exchange possibility and the water flowing through the gravels dilutes the leachate, the electrical conductivity decreases because the volume of water that dilutes the concentrated ions is greater. The conductivity then increases with depth because the amount of dissolved ions in solution increases over time. There is also seawater intrusion into the groundwater at depth and this will increase the total amount of dissolved ions in solution. The constituents of the groundwater will be different, containing more sodium, calcium and potassium than in the groundwater above.

When the electrical conductivity was logged over a period of time there were periodic cycles that occurred over a few hours but not always constant. They were much less frequent than the behaviour seen in the pH data. A change that was noted in the temporal data was that the electrical conductivity greatly increased on the 18th of June. This was not shown in the data before so is not related to the spring neap tidal cycling.

The temperature logging that occurred in ALO3 showed that there is an increase in the groundwater temperature and this is related to the warming up of the seasons. There were daily changes in the temperature that are affected by weather conditions at the time such as precipitation and the amount of sunshine received, so this will affect the amount of

water recharge. There were two time periods when the temperature changes were much greater than the daily fluctuations. These were from the 28th of May till the 2nd of June and the 14th of June until the 18th of June. These dates coincide with the occurrence of spring tides on the 25th of May and the 12th of June. This shows that the effect of the influx of more seawater on a spring tide increases the groundwater temperatures but there is a slight time delay.

Zinc and sodium were picked to act as indicators for the leachate pollution in the groundwater and the possible occurrence of seawater intrusion in the lower parts of the aquifer.

The zinc profiles that were obtained actively reflected the assumption that the lower pH values in the upper metres of the landfill were due to landfill leachate being produced. This led to the dissolution of more zinc. The concentrations were high in the landfill region and they decreased with depth because there was no known natural source for the zinc at 14m. The peaks in the concentrations at 4m and 6m in all the MLS boreholes must be due to either a source region that lies further inland at these depths and the dissolved ions are transported without downward movement of the water, or the hydraulic conductivity of the layer immediately below is lower and there is a concentrating of the dissolved zinc at that depth that flows with the natural groundwater towards the estuary. There are also troughs in the zinc concentrations at depths of 5m and 8m, which may be due to the geology of the aquifer. The clay region in MLSO2 is located at 5m depth so may be adsorbing some of the zinc ions.

There is a noticeable increase in the concentration of zinc in the upper metres of borehole MLSO3 that may be a possible indicator that a leachate plume is migrating towards the estuary. The analysis of the predominant groundwater flow direction shows that this may be the case.

Sodium was used as an indicator of the influx of saline water into the groundwater on land. This appeared to work because the concentrations greatly increased at depths of 12 to 14m depending on the borehole location. The seawater would have intruded along the clay-impeding layer. However, sodium experiences geochemical interactions between particle surfaces and other ions such as calcium and magnesium (Appelo, 1994). This means that the behaviour seen may not purely be due to the intrusion of seawater. This is also fair to assume seeing as there might be a saline influence from the nearby coastline. These geochemical interactions may be the cause of the higher sodium concentrations seen at depths of 7m in MLSO1 and MLSO3 and 7m and 8m in MLSO2.

6. Conclusion

It can be seen that there are complex processes occurring in the coastal aquifer, which have been complicated even more by the fact that there may be an influence of the nearby coastline on the groundwater flow. It appears that the groundwater flow is mostly affected by the tides from the coastline but that the estuary causes groundwater nearby to flow towards it rather than towards the coastline during low tides.

There does not appear to be a noticeable effect of the spring neap cycle on the groundwater chemistry of the system. This may be because there is not any effect or because the ions that were analysed were not able to detect these changes. The temperature data hinted at a spring tide effect increasing the groundwater temperatures and so the ions that were used here may not have been adequate to serve the purpose of fulfilling the aims.

It can be concluded that there is movement of a leachate plume towards the estuary because an increased concentration of pollutants was witnessed at MLSO3 over time. Therefore it is fair to say that there is a risk that pollution will be released into the estuary in the future. It may also be likely that a hollow that is located near borehole ALO3 may be acting as a drainage point for any leachate pollution nearby.

It is also noticeable that there are short-term changes in the temperature, pH and electrical conductivity that may be worth investigating and determining what they are caused by and may be affected by.

7. Errors and Improvements

Experimental Errors

These were errors that occurred during the measurements of values either in the field or in the laboratory that were either minimized as much as possible or were unavoidable. There were measurements in the field involving the use of loggers and probes that may not be effectively calibrated and so the values in electrical conductivity, pH and temperature for example may be skewed from the real values. The loggers may not be set at the correct date and time for when logging was carried out and adjustments may need to be made.

The loggers are battery powered and when these run out logging of data may become difficult. If the batteries expire before the next site visit then it is possible that data will be lost.

There were problems involved with the slug test analysis in borehole ALO3 that occurred because the slug was caught by the pressure transducer when the rising head test was carried out. This displaces the pressure transducer and also affects the assumption that the injection of the slug is instantaneous.

The analysis of the water samples in the laboratory are prone to errors in the results because the samples may become contaminated by equipment during any of the analysis, eg. Filtration, mixing of standards, testing of diluted samples. The AAS and EMS machines will also cause a standard error in the results which may be affected by drift in the machine.

Improvements

It was not identified that the flow direction of the groundwater was affected by the spring and neap tides. Therefore it is proposed that a head monitoring of spot measurements at half hourly intervals is carried out over a full tidal cycle, from high to high tide over a day for spring and neap tides to determine a more accurate picture of the groundwater flow patterns.

It may be worth logging the pH, electrical conductivity and temperature in ALO2 to determine whether there are greater effects evident in the data for the different tidal cycles because of the closer proximity to the coastline.

8. References

- Appelo C.A.J. (1994), Cation and proton-exchange, pH variations, and carbonate reactions in a freshening aquifer, *Water Resource Research*, 30, 2793-2805
- Bokuniewicz H. (1980), Groundwater seepage into Great South Bay, New York, *Estuarine and Coastal Marine Science*, 10, 437-444
- Butler J.J. Jr. (1998), The design, performance, and analysis of slug tests, USA: CRC Press LLC Lewis Publishers.
- Clements, J *Alfred Nobel* Retrieved October, 17th, 2002 from http://www.threetowners.com/Ardeer%20Factory/ardeer_factory.htm
- Dolan, J. E., (n.d.). *Nobel in Scotland*. Retrieved on March, 21st, 2002 from <http://www.nobel.se/nobel/alfred-nobel/industrial/dolan/>.
- Fetter, C. W., (2001). *Applied Hydrogeology*, 4th ed. New Jersey: Prentice Hall.
- Fuller C., Davis J.A., Coston J.A, and Dixon E. (1995), Characterization of metal adsorption variability in a sand and gravel aquifer, Cape Cod, Massachusetts, USA, *Journal of Contaminant Hydrology*, 22, 165-187
- Geo C., Ramsey M.H., and Thornton I. (2001), Buffering from secondary minerals as a migration limiting factor in lead polluted soils at historical smelting sites, *Applied Geochemistry*, 16, 1193-1199
- Hamilton-Taylor J., Giusti L., Davison W., Tych W., and Hewitt C.N. (1997), Sorption of trace metals (Cu, Pb, Zn) by suspended lake particles in artificial (0.005M NaNO₃) and natural (Esthwaite Water) freshwaters, *Colloids and Surfaces*, 120, 205-219
- Jurjovec J., Ptacek C.J., and Blowes D.W. (2002), Acid neutralization mechanisms and metal release in mine tailings: A laboratory column experiment, *Geochimica et Cosmochimica Acta*, 66, 9, 1511-1523
- Johnson R.H., Blowes D.W., Robertson W.D., and Lambor J.L. (2000), The hydrogeochemistry of the Nickel Rim mine tailings impoundment, Sudbery, Ontario, *Journal of Contaminant Hydrology*, 41, 49-80
- Klug H.P. and Alexander L.E. (1954), X-ray diffraction procedures for polycrystalline and amorphous materials, John Wiley & Sons: New York
- Li L., Barry D.A., Stagnatti F., and Parlange J.Y (1999), Submarine groundwater discharge and associated chemical input to a coastal sea, *Water Resource Research*, 35, 3253-3259
- Ludvigsen L., Albrechtsen H.-J., Heron G., Bjerg P.L., and Christensen T.H. (1998), Anaerobic microbial redox processes in a landfill leachate contaminated aquifer, (Grinsted, Denmark), *Journal of Contaminant Hydrology*, 33, 273-291
- Mcgregor R.G., Blowes D.W., Jambor J.L., and Robertson W.D. (1998), The solid-phase controls on the mobility of heavy metals at the Copper Cliff tailings area, Sidbury, Ontario, Canada, *Journal of Contaminant Hydrology*, 33, 247-271

- Moore W.S. (1999), The subterranean estuary: A reaction zone of groundwater and seawater, *Marine Chemistry*, 65, 111-125
- Ramirez-Munoz J. (1968), Atomic-absorption spectroscopy and analysis by atomic-absorption flame photometry, Amsterdam: Elsevier Publishing Company
- Rybicka E.H., Calmano W., and Breger A. (1995), Heavy metals sorption/desorption on competing clay minerals: an experimental study, *Applied Clay Science*, 9, 369-381
- Tett P. (n.d.) *Marine Biology: Water Layering and water movements*. Retrieved October 23, 2002 from http://www.oaerre.napier.ac.uk/users/p.tett/MB/MB2_01.html
- Thornton S.F., Tellam J.H., and Lerner D.N. (2000), Attenuation of landfill leachate by UK Triassic sandstone aquifer materials 1. Fate of inorganic pollutants in laboratory columns, *Journal of Contaminant Hydrology*, 43, 327-354
- Volker R.E., and Rushton K.R. (1982), An assessment of the importance of some parameters for seawater intrusion in aquifers and a comparison of dispersive and sharp interface modeling approaches, *Journal of Contaminant Hydrology*, 56, 239-250

Appendices

Appendix 1 – The completion of the MLS boreholes

The boreholes are multi-port sampling installations that consist of a bundle of nylon access tubing, of approximately 3.125mm outside diameter and a wall thickness of 0.48mm, of various lengths.

Each tube is connected at the base, by a short length of 'clear soft plastic', to a slotted PVC-covered aluminium screen of 10 to 20 cm length. The PVC tubing around the screen has an outside diameter of 6.35mm and a wall thickness of 0.91mm. The aluminium screen is covered by 'inert' nylon meshing, that is used to prevent clogging of the nylon tubing by biological matter.

A three-way nylon tap is at the external end of the nylon access tubing, which is removed when not sampling the borehole. An electrical conduit, approximately 16mm wide, is inserted between the bundle of tubing to provide rigidity and to straighten the tubing. (Enot, pers. comm. n.d.).

Appendix 2 – The completion of the AL Boreholes

Figure A1 shows the details of the ALO1, ALO2 and ALO3 boreholes.

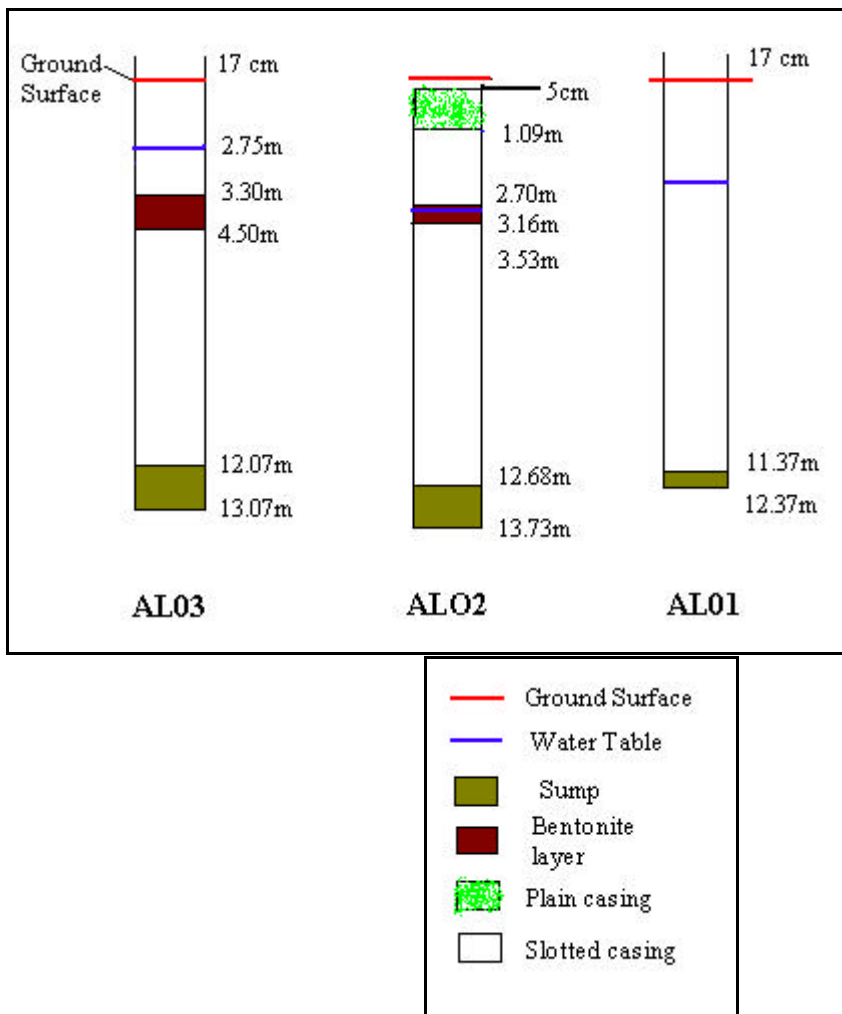


Figure A1: The finishing design of the AL boreholes

Appendix 3 – Previous data from the site Head Monitoring

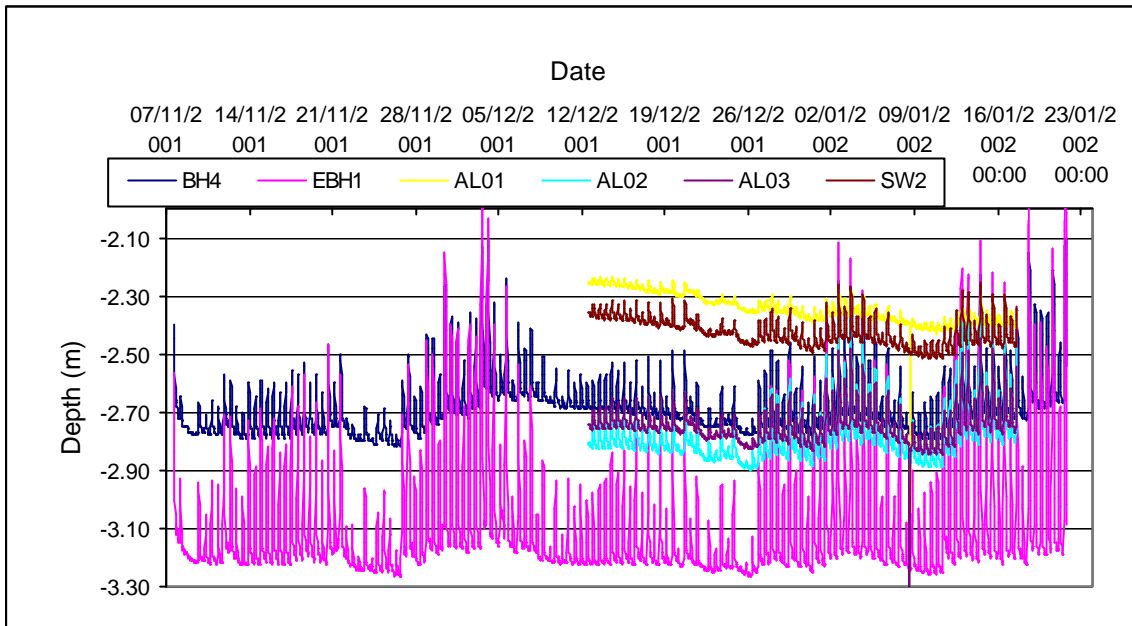


Figure A2: The temporal variations in the height of the water table in the boreholes (taken directly from Binley, pers. comm., n.d.).

Figure A1 shows that the nearer to the estuary the monitoring was carried out then the larger the amplitude of the variations in the water table height. EBH1 is the closest borehole to the estuary and AL01 is the furthest away.

Temperature monitoring

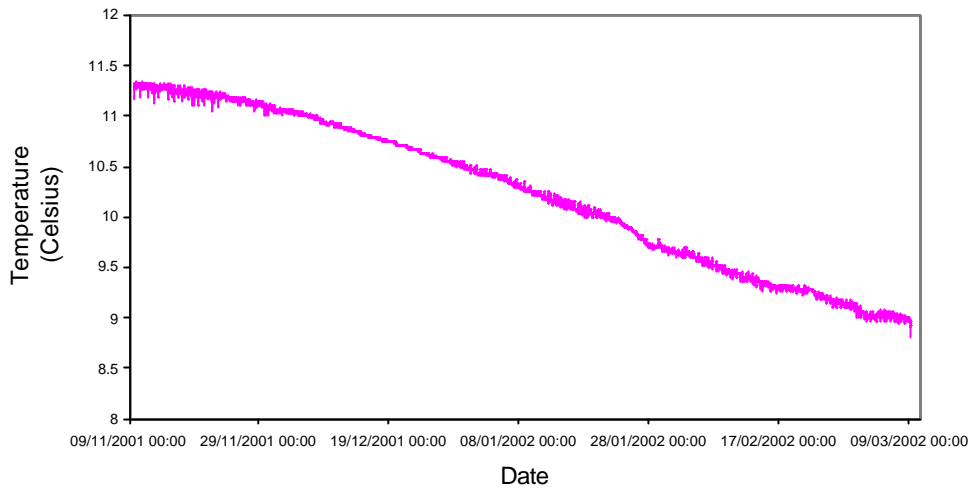


Figure 3: Temporal variations in the temperature in SW2

There is an overall downward trend in the logged data as the atmospheric temperatures decrease as well. This is a seasonal relationship.

Electrical conductivity monitoring

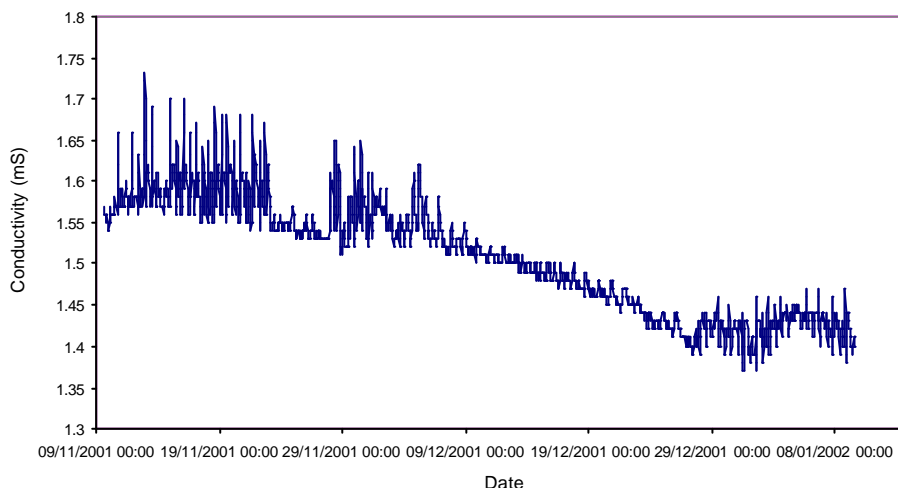


Figure 3: Temporal changes in the electrical conductivity of SW2

There appears to two cycles in the data. There is a diurnal cycle in the electrical conductivity, related to the influx of saline water and then refreshing of the aquifer by freshwater. A seasonal cycle appears to be acting on the electrical conductivity because there is an overall downward trend in the values found.

Appendix 4 – Sampling and Filtration Methods
Sampling of the MLS boreholes

- Attach a new 50-60ml disposable syringe to the three-way tap system and then attach to the access tubing for Port Number 1 in MLSO1. The number of ports and their depths for each borehole are shown in Table 4. Record the start time of sampling.

Table 4: The MLS boreholes and their number of sampling ports with their corresponding depths. a) MLSO1 b) MLSO2 c) MLSO3

(a)		(b)		(c)	
Port No.	Depth (m)	Port No.	Depth (m)	Port No.	Depth (m)
1	-2.4	1	-4.3	1	-4.5
2	-2.9	2	-4.8	2	-5
3	-3.4	3	-5.3	3	-5.5
4	-3.9	4	-5.8	4	-6
5	-4.4	5	-6.3	5	-6.5
6	-4.9	6	-6.8	6	-7
7	-5.4	7	-7.3	7	-7.5
8	-5.9	8	-7.8	8	-8
9	-6.4	9	-8.3	9	-8.5
10	-6.9	10	-8.8	10	-9.5
11	-7.4	11	-9.8	11	-10.5
12	-7.9	12	-10.8	12	-11.5
13	-8.4	13	-11.8	13	-12.5
14	-9.4	14	-12.8		
15	-10.4	15	-13.3		
16	-11.4				
17	-12.4				
18	-13.4				
19	-14.4				
20	-15.4				

- Using the plunger on the syringe, remove 100ml of water from the nylon access tubing into the syringe. This water has remained in the tubing since the last

sampling session and does not provide an accurate sample of the groundwater at that specific depth. Using the 3-way tap, release the initial 50ml of water into a plastic 100ml beaker and then extract a further 50ml. Rinse the beaker out using this water and discard.

- Sample a further 100ml of water from the borehole using the above method and retain this sample in the beaker. Using the pH, temperature and electrical conductivity probes measure and record their respective values.
- Pour 50ml of sample into two separate Nalgene sample bottles and label with the date of sampling, the port number and the borehole name.
- Do this for all the ports in the MLSO1 borehole that will yield a sample and record the finish time of sampling.
- Then sample MLSO2 and MLSO3, recording the start and finish time of sampling, the temperature, electrical conductivity and the pH for each sample.

Filtration method for the water samples

- Two normal filter units, consisting of two conical flasks, two porcelain funnels and Whatman 40 paper filets, were set-up using the laboratory pumps. The conical flask is connected to the pump using the rubber tubing.
- The porcelain funnel was then connected to the conical flask using a bung, to maintain the suction created and increase the speed of the filtering.
- A paper filet was inserted into the porcelain funnel and dampened, using some of the sample that was to be filtered. This sealed the suction and the rest of the sample (the two corresponding 50ml bottles) was added to the funnel for filtration. The sample bottles were rinsed with de-ionized water and allowed to drain.
- When the filtration was complete, the tubing connecting the pump to the conical flask was removed. Then the porcelain funnel and the Whatman filter filet were removed. The funnel was rinsed with de-ionized water and allowed to drain.
- The sample bottles were refilled with the filtered water from the conical flask and then two drops of 0.1M Nitric Acid were added and the lids were replaced. This prevents any sorption of metals onto the walls of the sample bottle. The conical flask was rinsed with de-ionized water and allowed to drain.
- Repeat this method for all the pairs of samples.

The samples were then placed in a cooler box for transport and then chilled until they were to be analyzed.

Appendix 5 – Analytical methods used for AAS and EMS

Atomic Absorption Spectroscopy

The analytical concentration range that the AAS machine works accurately between is 0-1ppm (parts per million).

The concentration of the zinc standard solution was diluted from 100ppm to 10ppm initially using de-ionized water. From the 10ppm standard, six different standards were created, ranging between 0ppm and 1ppm. These standards were added to 100ml volumetric Pyrex flasks using a 10ml pipetter, labeled and made up to volume using de-ionized water.

The standards were then analyzed using the atomic absorption spectrometer first, in order to obtain a calibration graph. Three samples were taken automatically and the results and the standard deviation, calculated from three samples by the machine, were recorded. The samples from the boreholes were analyzed from the Nalgene bottles and any concentrations higher than the top calibration point were set aside for dilution.

Dilutions were made using 100ml and 50ml volumetric Pyrex flasks, depending on availability, and made up to volume using de-ionized water. These were then analyzed using the atomic absorption spectrometer and the results with their corresponding standard deviations were recorded.

The calibration graph was then used to calculate the concentration of zinc in each sample. Any dilutions were then inverted and multiplied to the corresponding concentration found using the calibration graph.

Flame Emission Spectroscopy

The analytical concentration range that the EMS machine works most accurately between is 0-4ppm.

The initial concentration of the sodium standard was 1000ppm Na and this was used to create a 100ppm standard solution. From the 100ppm standard, five different standards were created by adding 0, 1, 2, 3 and 4ml of solution to five separate 100ml volumetric flasks and making up to the top with demonized water.

The EMS machine was allowed to warm up for a few minutes before any analysis was carried out in order to avoid the instability in the machine that occurs as the lamp warms up. The blank dial on the machine was used to calibrate the standards. The 0ppm standard was set to zero on the scale from 0-100 in the machine. The top standard, 4ppm, was then set to 100. The other samples were analysed and the readings recorded.

The samples were then analysed and because the concentrations were so high the dilutions were carried out using 25ml plastic cups. The total sample volume ranged from

3-5ml, depending on the dilution factors required. Automatic pipettors of 2-5 μ m, 0-10 μ m, 1ml and 10ml pipettors were used to carry out the dilutions. Samples were made up to volume with deionised water. Contamination of samples was avoided by discarding the pipettor tips after use of that sample was finished.

The readings were recorded and a calibration graph was produced. The concentrations of sodium were found from the graph and then multiplied by the inverse of the dilution factor to get the total concentration in the sample.

Appendix 6 – Correction details

Table 5: Borehole heights and dip corrections relative to ground level at BH4

Borehole	Height corrections	Casing Height	Net dip correction
BH4	0	0.32	-0.32
SW2	+0.214	0	-0.214
ALO1	-0.048	0.21	-0.162
ALO2	+0.441	0.11	-0.551
ALO3	+0.196	0.19	-0.386

Table 6: Coordinates of the boreholes using a designed coordinate system

Borehole	X	Y
BH4	136.842	307.519
SW2	106.015	264.662
ALO1	63.881	281.65
ALO2	188.46	257.52
ALO3	164.47	234.63
MLSO1	111.23	262.65
MLSO2	155.61	274.45
MLSO3	173.78	275.82

